

Dynamin-mediated Internalization of Caveolae

John R. Henley,* Eugene W.A. Krueger,[§] Barbara J. Oswald,[§] and Mark A. McNiven*^{‡§}

*Department of Molecular Neuroscience, [‡]Department of Biochemistry and Molecular Biology, and [§]Center for Basic Research in Digestive Diseases, Mayo Clinic, Rochester, Minnesota 55905

Abstract. The dynamins comprise an expanding family of ubiquitously expressed 100-kD GTPases that have been implicated in severing clathrin-coated pits during receptor-mediated endocytosis. Currently, it is unclear whether the different dynamin isoforms perform redundant functions or participate in distinct endocytic processes. To define the function of dynamin II in mammalian epithelial cells, we have generated and characterized peptide-specific antibodies to domains that either are unique to this isoform or conserved within the dynamin family. When microinjected into cultured hepatocytes these affinity-purified antibodies inhibited clathrin-mediated endocytosis and induced the formation of long plasmalemmal invaginations with attached clathrin-coated pits. In addition, clusters of

distinct, nonclathrin-coated, flask-shaped invaginations resembling caveolae accumulated at the plasma membrane of antibody-injected cells. In support of this, caveola-mediated endocytosis of labeled cholera toxin B was inhibited in antibody-injected hepatocytes. Using immunoisolation techniques an anti-dynamin antibody isolated caveolar membranes directly from a hepatocyte postnuclear membrane fraction. Finally, double label immunofluorescence microscopy revealed a striking colocalization between dynamin and the caveolar coat protein caveolin. Thus, functional *in vivo* studies as well as ultrastructural and biochemical analyses indicate that dynamin mediates both clathrin-dependent endocytosis and the internalization of caveolae in mammalian cells.

EUKARYOTIC cells internalize plasma membrane, surface receptors, and small molecules via several distinct endocytic processes (reviewed in Anderson et al., 1992; Anderson, 1993c; Goldstein et al., 1985; Watts and Marsh, 1992; van Deurs et al., 1993; Sandvig and van Deurs, 1994; Lamaze and Schmid, 1995). The most characterized process is receptor- or clathrin-mediated endocytosis (Anderson et al., 1977; Goldstein et al., 1979), which uses a clathrin and adaptor protein complex to sequester receptors and associated ligands into 100–150-nm-diam coated pits at the plasma membrane (reviewed in Goldstein et al., 1985; Pearse and Robinson, 1990). Recently, a more enigmatic endocytic process has been studied whereby cells internalize certain glycosylphosphatidylinositol (GPI)¹-linked proteins, albumin, bacterial toxins, class I human leukocyte antigen (HLA), viruses, and small proteins (e.g., Huet et al., 1980; Kartenbeck, et al., 1989; Parton et al., 1994; Predescu et al., 1994, 1997; Schnitzer et al., 1994, 1996; Smart et al., 1994, 1995; Stang et al., 1997). This pathway, which is clearly distinct from clathrin-mediated

endocytosis, relies on flask-shaped, nonclathrin-coated, 50–85-nm-diam plasmalemmal vesicles called caveolae (e.g., Palade, G.E. 1953. *J. Appl. Physics*. 24:1424 (Abstr.); Palade and Bruns, 1968; Rothberg et al., 1992; Yamada, 1955). The molecular mechanisms by which these distinct plasmalemmal invaginations are severed to produce endocytic vesicles both require GTP hydrolysis, yet remain largely undefined (Carter et al., 1993; Schnitzer et al., 1996). Whereas the dynamins have been implicated in the scission of clathrin-coated vesicles from the plasma membrane (Takei et al., 1995; reviewed in De Camilli et al., 1995), it is unknown how caveolae and noncoated plasmalemmal invaginations detach to form free endocytic vesicles.

The dynamins are a multigene family of large (100-kD) GTPases that were originally identified in the brain (Shpetner and Vallee, 1989) and, more recently, have been implicated in endocytosis (reviewed in De Camilli et al., 1995; Robinson et al., 1994; Urrutia et al., 1997; Warnock and Schmid, 1996). Seminal studies on the paralytic *shibire*^{ts1} mutants of *Drosophila melanogaster* (Grigliatti et al., 1973), which express a temperature-sensitive mutation in the GTP-binding domain of the fly dynamin (Chen et al., 1991; van der Bliek and Meyerowitz, 1991), revealed dramatic ultrastructural alterations of the plasma membrane in both neuronal and epithelial cells (reviewed in Urrutia et al., 1997). At the restrictive temperature, nerve termi-

Please address all correspondence to Mark A. McNiven, Center for Basic Research in Digestive Diseases, Mayo Clinic, Rochester, MN 55905. Tel.: (507) 284-0683. Fax: (507) 284-0762. E-mail: mcniven.mark@mayo.edu

1. *Abbreviations used in this paper:* Dyn1/2/3, dynamin I/II/III; GPI, glycosylphosphatidylinositol; HLA, human leukocyte antigen; pIgA-R, polymeric IgA receptor.

nals of paralyzed flies are depleted of synaptic vesicles and accumulate short, nonclathrin-coated, "collared" pits at the plasma membrane, consistent with a defect in the endocytic retrieval of synaptic vesicle membrane (Koenig and Ikeda, 1989; Kosaka and Ikeda, 1983a; Poodry and Edgar, 1979). In contrast, epithelial cells of paralyzed flies contain numerous long plasmalemmal invaginations attached to clathrin-coated pits, suggesting an impairment of clathrin-mediated endocytosis (Kessel et al., 1989; Koenig and Ikeda, 1990; Kosaka and Ikeda, 1983b). These observations are supported by more recent studies on mammalian cells overexpressing a mutant dynamin, in which clathrin-mediated endocytosis is impaired (Herskovitz et al., 1993; van der Blik et al., 1993; Damke et al., 1994, 1995), leading to the formation of long plasmalemmal invaginations that are similar to those observed in epithelial cells from the *shibire^{ts1}* mutants (Damke et al., 1994). Further characterization of these transfected cells showed that fluid-phase endocytosis is not inhibited (Herskovitz et al., 1994; Damke et al., 1994) but upregulated over time, possibly to compensate for the inhibition of clathrin-mediated endocytosis (Damke et al., 1995). This change in fluid-phase endocytosis is particularly surprising when compared with cells of the *shibire^{ts1}* mutants, in which both clathrin-mediated endocytosis and fluid-phase endocytosis are inhibited at the restrictive temperature (Kessel et al., 1989; Kosaka and Ikeda, 1983a,b). Thus, it is currently unclear whether the dynamins participate solely in one or several endocytic processes. It has been hypothesized that multiple dynamin isoforms may perform a variety of endocytic functions (Artalejo et al., 1995; Urrutia et al., 1997).

Three distinct dynamin genes have been identified in mammals. Dynamin I (Dyn1) is expressed exclusively in neurons (Obar et al., 1990), dynamin II (Dyn2) is found in all tissues (Cook et al., 1994; Sontag et al., 1994), and dynamin III (Dyn3) is restricted to the testis, the brain, the lung, and the heart (Cao, H., and M.A. McNiven, manuscript in preparation; Cook et al., 1996; Nakata et al., 1993). Each dynamin gene encodes four or more alternatively spliced isoforms (reviewed in Robinson et al., 1994; Urrutia et al., 1997). Thus, all cells coexpress at least four Dyn2 isoforms, and neurons may express 12 or more distinct dynamins. Additional unidentified dynamin family members are likely to exist as well. It is unclear if the different dynamin gene products perform redundant functions or participate in distinct endocytic processes. To date, the important studies on cultured mammalian cells have overexpressed a mutant Dyn1 isoform in epithelial cells that do not normally express Dyn1 but rather four isoforms of Dyn2 (Damke et al., 1994, 1995; Herskovitz et al., 1993; van der Blik et al., 1993). Therefore, the resulting phenotype that is observed in these cells may provide only a partial view of the cellular processes in which the endogenous dynamins are involved.

The focus of this study was to extend the observations described above and define the function of a single dynamin family member in mammalian epithelial cells. To this end, we generated antibodies to peptides representing a conserved domain of the dynamin family and to a second region that is specific to the ubiquitously expressed Dyn2. Our goal was to test the effects of these affinity-purified antibodies on distinct endocytic processes and plasmalem-

mal morphology when injected into cultured mammalian epithelial cells. We found that two of these anti-dynamin antibodies inhibited the cellular uptake of fluorescent transferrin conjugates and induced the formation of long clathrin-coated invaginations from the plasma membrane, consistent with the *shibire^{ts1}* phenotype and the observations from epithelial cells overexpressing a mutant Dyn1 isoform. In addition to these long clathrin-coated membranes in the anti-dynamin antibody-injected cells, we observed numerous, nonclathrin-coated, flask-shaped structures resembling caveolae that accumulated at the plasma membrane. The density of these plasmalemmal invaginations was increased significantly in the anti-dynamin antibody-injected cells compared with controls. Strikingly, these caveolar profiles frequently formed large, aberrant, grape-like clusters that extended deep within the cytoplasm. To determine if these structures represented a perturbation of normal caveolar function, we showed that the internalization of fluorescein-labeled cholera toxin B (FITC-cholera toxin B), which normally is mediated by caveolae, was inhibited in anti-dynamin antibody-injected cells. Electron microscopy confirmed that HRP-labeled cholera toxin B (HRP-cholera toxin B) remained concentrated in plasmalemmal caveolae in these inhibited cells and did not gain access to cytoplasmic organelles. To verify that dynamin associates with caveolae, an anti-dynamin antibody was used to immunoprecipitate caveolar membranes from a subcellular postnuclear membrane fraction. In addition, double label immunofluorescence microscopy of cultured hepatocytes revealed a significant overlap between dynamin and caveolin. These results demonstrate that Dyn2 participates in an additional endocytic process that is distinct from clathrin-mediated endocytosis and provide insight into the molecular mechanisms governing the GTP-mediated internalization of caveolae.

Materials and Methods

Cell Culture

A normal mouse hepatocyte cell line (BNL CL2; Patek et al., 1978) from American Type Culture Collection (Rockville, MD) was maintained in DME containing 4.5 g/liter glucose and 10% FBS (GIBCO BRL, Gaithersburg, MD). These nonpolarized cells make albumin but, unlike hepatocytes in situ, express high levels of caveolin and only trace amounts of the polymeric IgA receptor (pIgA-R; data not shown, but see Fig. 9). Cells were grown in plastic culture flasks for biochemical analyses, on acid-washed coverglasses for fluorescence microscopy, and on carbon-coated and glow-discharged gridded coverglasses (Bellco Glass, Inc., Vineland, NJ) for electron microscopy.

Antibodies and Reagents

Polyclonal anti-peptide antibodies to dynamin were generated in rabbits and affinity purified as described previously (Henley and McNiven, 1996). The anti-Pan61 and anti-Pan65 antibodies were made to peptide sequences representing amino acids 262–292 and 223–249 of Dyn1, respectively (see Fig. 1 a), which are conserved among the known mammalian dynamin isoforms (Cook et al., 1994; Nakata et al., 1993; Obar et al., 1990; Sontag et al., 1994). The anti-Dyn2T antibody was raised against a peptide sequence representing amino acids 761–785 of Dyn2 (see Fig. 1 a), which is unique to the four Dyn2 isoforms, sharing only 20–26% identity with the other dynamin gene products (Cook et al., 1994; Sontag et al., 1994). The polyclonal isoform-specific anti-Dyn1, anti-kinesin, and anti-pIgA-R antibodies have been described (Henley and McNiven, 1996). Monoclonal anti-caveolin antibodies were purchased from Transduction Laboratories (Lexington, KY) and Zymed Laboratories, Inc. (South San Francisco,

CA). A polyclonal antibody to the β_1 subunit of the Na^+/K^+ ATPase was from Upstate Biotechnology Inc. (Lake Placid, NY), as was a goat anti-rabbit IgG Fc antibody. Secondary goat anti-rabbit and goat anti-mouse IgG antibodies linked to HRP were from Tago, Inc. (Burlingame, CA). Fluorescein- and Texas red-labeled dextrans (3 kD, lysine fixable), fluorescent conjugates of human transferrin, and Cascade blue hydrazide (dilithium salt) were from Molecular Probes, Inc. (Eugene, OR), as were the SlowFade and ProLong antifade reagents. A monoclonal antibody to α -adaptin as well as FITC- and HRP-cholera toxin B were from Sigma Chemical Co. (St. Louis, MO).

Subcellular Fractionation, Immunoprecipitation, Immunoisolation, and Western Blot Analysis

Livers were isolated from male Sprague Dawley rats (Harlan Sprague Dawley Inc., Indianapolis, IN) and homogenized at 2,800 rpm with a Potter-Elvehjem type homogenizer after adding 3 vol of 4°C Buffer A (10 mM Hepes, pH 7.2, 25 mM sucrose, and 10 mM EGTA) containing protease inhibitors (1 mM phenylmethylsulfonyl fluoride, 100 $\mu\text{g}/\text{ml}$ soybean trypsin inhibitor, 10 $\mu\text{g}/\text{ml}$ leupeptin, 10 $\mu\text{g}/\text{ml}$ *p*-toluenesulfonyl-L-arginine methyl ester, and 5 $\mu\text{g}/\text{ml}$ pepstatin A). The homogenate was centrifuged 15 min at 13,000 g then 1 h at 100,000 g, and the supernatant was collected as the cytosolic fraction. This cytosolic fraction was subjected to SDS-PAGE and Western blot analysis.

For immunoprecipitations, brains from male Sprague Dawley rats were homogenized as described above in 4 vol of 4°C RIPA buffer (50 mM Tris, pH 8.0, 150 mM NaCl, 1 mM EDTA, 1% Triton X-100, 0.5% deoxycholate, and 0.1% SDS) containing protease inhibitors. The homogenate was centrifuged as above and the supernatant collected as the clarified extract. Appropriate antibodies (5 μg) were incubated with 1-ml fractions (15–25 mg) of the clarified extracts, and then preswollen protein A beads (5 mg) were added before a second incubation. Incubations were 2–12 h at 4°C with rotation. Beads and immune complexes were collected by centrifuging 3 min at 7,000 g and then rinsed 4 \times 5 min with the starting buffer before being subjected to SDS-PAGE and Western blot analysis.

Immunoisolations were done as reviewed by Howell et al. (1989). To prepare the starting membrane fraction, confluent cultures of hepatocytes (~600 cm^2) were scraped into 4°C buffer A containing protease inhibitors and homogenized by sonication. The homogenate was centrifuged 10 min at 1,000 g to obtain a postnuclear supernatant that then was centrifuged 1 h at 100,000 g to collect the pellet as the postnuclear membrane fraction. This postnuclear membrane fraction was resuspended gently in PBS-FBS (8.1 mM NaH_2PO_4 , 1.2 mM KH_2PO_4 , pH 7.2, 138 mM NaCl, 2.7 mM KCl, 2 mM EDTA, 0.9 mM CaCl_2 , 0.5 mM MgCl_2 , and 5% FBS). Affinity-purified anti-Pan61 antibody, or the anti-pIgA-R antibody as a control, were linked to Dynabeads M-500 Subcellular superparamagnetic beads (DynaL, Inc., Lake Success, NY) as described previously (Henley and McNiven, 1996). The appropriate antibody-coated beads (10 mg) and 0.5–2.0 mg of the starting membrane fractions were incubated ~8 h at 4°C with rotation in 1 ml of PBS-FBS. The beads and any bound membranes then were collected with a magnet, rinsed three times with PBS-FBS, and subjected to SDS-PAGE and Western blot analysis.

The protein concentration of each cellular extract was determined using bicinchoninic acid, as per instructions from the manufacturer (Pierce Chemical Co., Rockford, IL). For Western blot analysis, cellular protein extracts and immune complexes were reduced in sample buffer (62.5 mM Tris, pH 6.8, 5% glycerol, 4% β -mercaptoethanol, 2% SDS, and 4 $\mu\text{g}/\text{ml}$ bromophenol blue), separated by discontinuous SDS-PAGE (Laemmli, 1970) and electrophoretically transferred to polyvinylidene difluoride filters (Towbin et al., 1979). Filters containing transferred proteins were incubated with appropriate primary antibodies (0.5–1 $\mu\text{g}/\text{ml}$) and then HRP-conjugated secondary antibodies (0.5–1 $\mu\text{g}/\text{ml}$), as reported previously (Henley and McNiven, 1996). Reactive bands were visualized by exposing the filters to autoradiographic film (Eastman Kodak Co., Rochester, NY) after using enhanced chemiluminescence detection reagents (Amersham Corp., Arlington Heights, IL) as per instructions from the manufacturer. Developed autoradiographs were subjected to densitometric analysis using a Bio-Rad imaging densitometer (Model GS-700) and Molecular Analyst software (Bio-Rad Laboratories).

Microinjections

Microinjections were done on a 37°C microscope stage and cells were allowed to recover 2–6 h before subsequent manipulations. Cells were pressure injected using an IM-200 microinjector system (Narishige USA, Inc.,

Greenvale, NY) and microneedles that were pulled from thin-wall (1.0-mm outer diam; 0.78-mm inner diam) borosilicate tubing (with filament) using a Flaming/Brown P-97 micropipette puller (Sutter Instrument Co., Novato, CA). Injected antibodies were purified anti-Pan65, anti-Dyn2T, or irrelevant anti-kinesin antibodies that were dialyzed and concentrated (2–15 mg/ml) in microinjection buffer (10 mM KH_2PO_4 , pH 7.2, and 75 mM KCl) using 30-kD molecular mass cut off Nanosep Microconcentrators (Pall Filtron Corp., Northborough, MA). For additional control injections, the anti-Pan65 and anti-Dyn2T antibodies were heat inactivated by incubating 5 min at 100°C. Cascade blue hydrazide (2.5 mM) or fluorescent dextran conjugates (400 μM) were added to all microinjection solutions. This served as an indicator for successful microinjections and enabled injected cells to be identified readily by fluorescence microscopy after functional assays were performed. For experiments where electron microscopy would be used, it was necessary to inject every cell within a particular square (1 mm^2) of the gridded coverglass. In some of these experiments colloidal gold (5-nm diam) was included in the injection solution to identify injected cells by electron microscopy.

Functional Assays

As a measure of clathrin-mediated endocytosis, the cellular internalization of rhodamine-, fluorescein-, or Texas red-labeled transferrin was assayed. First, cells were rinsed with 37°C HBSS (Sigma Chemical Co.) and incubated in DME containing 2% defatted BSA (DME-BSA) to remove unlabeled transferrin. Cells then were incubated 15 min at 37°C in DME-BSA containing 5 $\mu\text{g}/\text{ml}$ of an appropriate fluorescent transferrin conjugate to allow internalization. Finally, cells were rinsed twice with 4°C DME-BSA (adjusted to pH 3.5 with acetic acid) and four times with HBSS to remove surface labeling and then processed for fluorescence microscopy.

To assay caveola-mediated endocytosis, the internalization of FITC- or HRP-cholera toxin B was monitored by fluorescence or electron microscopy, respectively. Cells were rinsed with HBSS and incubated in DME-BSA as above, then chilled to 4°C and incubated 15 min in DME-BSA containing 4 $\mu\text{g}/\text{ml}$ FITC- or HRP-cholera toxin B. Labeled cells were rinsed four times with 4°C HBSS to remove unbound toxin. These cells then were incubated ~2.5 h in DME-BSA at 37°C to allow internalization and appropriately fixed. For double labeling experiments, 5 $\mu\text{g}/\text{ml}$ Texas red-labeled transferrin was included during the last 15 min of the 2.5 h internalization incubation at 37°C before rinsing the cells as in the assay for clathrin-mediated endocytosis.

Fluorescence Microscopy

Labeled cells were rinsed briefly with 37°C PBS (8.1 mM NaH_2PO_4 , 1.2 mM KH_2PO_4 , pH 7.2, 138 mM NaCl, 2.7 mM KCl, 0.9 mM CaCl_2 , and 0.5 mM MgCl_2), submerged in 37°C fixative (100 mM Pipes, pH 6.95, 3 mM MgSO_4 , 1 mM EGTA, and 2.5% formaldehyde) and incubated 20 min at room temperature. For indirect immunocytochemistry, fixed cells were permeabilized with PBS containing 0.1% Triton X-100 and then incubated with antibodies as described (Henley and McNiven, 1996). Cells were rinsed three times with PBS and once with distilled water, then they were mounted in SlowFade or ProLong antifade reagents. Digital images were acquired using an intensified charged coupled device camera (XC-77; Hamamatsu Photonics K.K., Hamamatsu City, Japan) or a cooled charged coupled device camera (SenSys; Photometrics, Tucson, AZ) attached to a Zeiss Axiovert 35 microscope that was equipped with a mercury arc (50 or 100 W). A laser scanning confocal microscope (LSM-410; Carl Zeiss, Inc.) also was used. Acquired images were manipulated with Image-1 and Metamorph software (Universal Imaging Corp., West Chester, PA) then stored on a computer hard drive. Alternatively, photographic images were recorded on Kodak film (Ektachrome, 400 ASA or Tmax, 3200 ASA) using a 35-mm camera attached to the microscope, and the images were digitized using a Sprint-Scan 35 slide scanner (CS-2700; Polaroid Corp., Cambridge, MA) and Adobe Photoshop software (Adobe Photosystems, Inc., Mountain View, CA).

Electron Microscopy

For conventional electron microscopy, cells were rinsed with 37°C PBS, submerged in 37°C primary fixative (100 mM cacodylate, pH 7.4, 60 mM sucrose, 2.5% glutaraldehyde) and incubated 1 h at room temperature. Cells then were incubated 1 h at room temperature in 1% osmium tetroxide. Fixed cells subsequently were incubated 1 h at room temperature in 1% uranyl acetate, dehydrated in a graded series of ethanol, and embedded in Quetol 651 (Ted Pella, Inc., Redding, CA). To make the plasma

membrane electron dense, 1 mg/ml ruthenium red was included in the primary fixative and in the 1% osmium tetroxide solution, and cells were osmicated an additional 2 h. For the cytochemical detection of HRP, cells were rinsed, incubated 30 min in the fixative (100 mM cacodylate, pH 7.4, 100 mM sucrose, 0.5% glutaraldehyde) and then reacted with 1 mg/ml diaminobenzidine and 0.012% hydrogen peroxide for 15 min. Cells then were rinsed, incubated 1 h in 1% osmium tetroxide and 1.5% potassium ferricyanide and processed for electron microscopy as above.

After the embedding, the carbon interface enabled the underlying gridded coverglass to be separated readily from the embedded cells, leaving an imprint of the grid on the block face. This allowed the block face to be trimmed so that only the 1-mm² square containing the injected cells remained. Thin sections (0.09–0.1 μm) were cut parallel to the ventral surface of the cells using a diamond knife (Diatome U.S., Fort Washington, PA) and an Ultracut E microtome (Reichert-Jung, Wien, Austria). Sections were collected on copper grids, post-stained with lead citrate and viewed at ~60 kV with a JEOL 1200 transmission electron microscope (JEOL USA, Peabody, MA).

Quantitative and Statistical Analyses

All quantitation and stereology were done in a blinded fashion using standard techniques. The results presented (see Figs. 3 and 7; Tables I and II) are averages of data sets that were obtained by at least two of the authors who conducted these experiments in parallel. Quantitation of plasmalemmal invaginations and the surface density of caveolae was performed on electron micrographs of entire cell profiles. Micrographs were printed at a magnification of 4,000–12,000. To quantify the amount of invaginated plasma membrane, an overlay grid was used to count the number of points falling on ruthenium red-stained membranes relative to the number of points within the confines of the cell. A hand held magnifier (3×) aided in the identification of internal ruthenium red-stained membranes. Caveolae were defined by morphological criteria as plasmalemmal vesicles between 50 and 80 nm in diameter that lacked any obvious cytoplasmic coats. To determine the surface density of caveolae, we counted the number of ruthenium red-stained caveolae per cell that were within 50 nm of the plasma membrane. The perimeter of each cell then was traced on a digitizing pad and converted to micrometers using an NIH Image 1 software package (National Institutes of Health, Bethesda, MD). From these values we calculated the number of caveolae/μm²/cell. Results from the studies are expressed as the median ± SEM for each data set. Significance levels were determined by the Wilcoxon rank sum statistical analysis, as described in the footnotes to Tables I and II.

For quantitation of the functional assays by fluorescence microscopy, injected hepatocytes were identified by the distinctive fluorescence of the injectate. The injected cells then were scored as uninhibited when the fluorescence of the appropriate ligand was detected within the fixed cell or, alternatively, they were scored as inhibited when internal fluorescence could not be detected. Results from these experiments were expressed as the percentage of injected cells that were uninhibited and are presented as the mean of observations made on >45 cells for each solution injected, as described in the figure legends.

Results

Characterization of Anti-dynamin Antibodies

In this study we have used peptide-specific antibodies to define the function of Dyn2 *in vivo*. Fig. 1 *a* shows a schematic representation of Dyn2 and the regions and peptide sequences to which three different polyclonal antibodies were made. The regions designated Pan61 and Pan65 are located within the NH₂-terminal enzymatic domain that is conserved among all of the known dynamin isoforms, yet are distinct from other GTP-binding proteins. The third region, Dyn2T, is within the proline-rich COOH-terminal tail and is unique to Dyn2. For control experiments, we used an antibody to the microtubule-based motor enzyme kinesin (Vale et al., 1985) that shares some sequence homology to dynamin within the nucleotide-binding domain (Obar et al., 1990). Each of the anti-dynamin antibodies

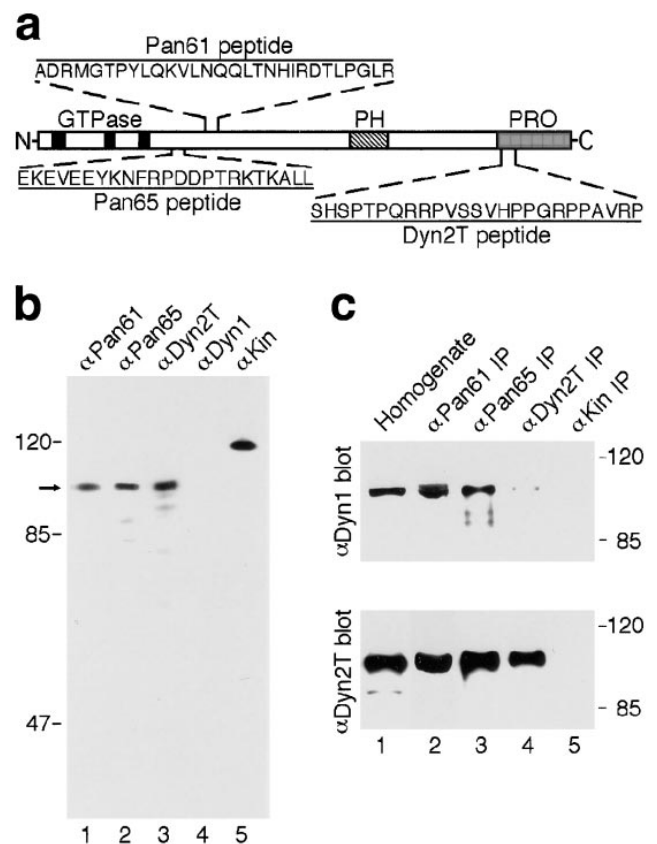
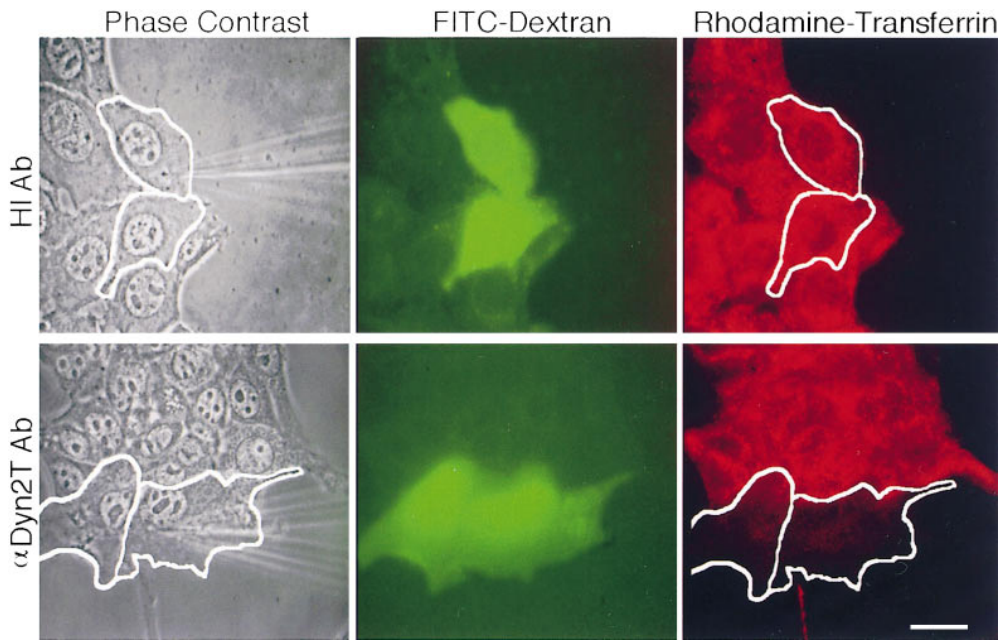


Figure 1. Characterization of dynamin-specific antibodies. (a) Diagram depicting the portions of dynamin to which anti-peptide antibodies were made. Two regions (*Pan61* and *Pan65*) are located within the NH₂-terminal “head” domain near the last of three GTP-binding elements (*black boxes*) and are conserved among the different dynamin isoforms. A third region (*Dyn2T*) is located within the proline-rich COOH-terminal “tail” domain (*PRO, shaded region*) and is unique to Dyn2. The location of the pleckstrin homology domain is indicated (*PH, striped box*). (b) Antibodies to the Pan61, Pan65, and Dyn2T peptides react with dynamin specifically by Western blot analysis. A cytosolic fraction was prepared from rat liver and then subjected to SDS-PAGE and Western blot analysis using the anti-Pan61 (lane 1), anti-Pan65 (lane 2), and anti-Dyn2T (lane 3) antibodies, or polyclonal antibodies that are specific for Dyn1 (lane 4) and kinesin (lane 5) as controls. A prominent dynamin band at ~100 kD (*arrow*) was detected with the anti-Pan61, anti-Pan65, and anti-Dyn2T antibodies but not with the anti-Dyn1 antibody, since Dyn1 is not expressed in epithelial tissues. The anti-kinesin antibody recognized a characteristic ~120-kD band. The positions of molecular mass standards are on the left. (c) The anti-Pan61 and anti-Pan65 antibodies immunoprecipitate both Dyn1 and Dyn2 from rat brain, whereas the anti-Dyn2T antibody is specific for Dyn2. Dynamin was immunoprecipitated from a crude brain homogenate (lane 1) using affinity-purified anti-Pan61 (lane 2), anti-Pan65 (lane 3), and anti-Dyn2T (lane 4) antibodies. Control immunoprecipitates were obtained with the anti-kinesin antibody (lane 5). The starting brain homogenate and subsequent immune complexes were subjected to SDS-PAGE and Western blot analysis with either a Dyn1-specific antibody (*top*) or the anti-Dyn2T antibody (*bottom*). Both Dyn1 and Dyn2 precipitated with the anti-Pan61 and anti-Pan65 antibodies, whereas the anti-Dyn2T antibody precipitated Dyn2 specifically, with only trace amounts of Dyn1 detected.



fluorescence of the dextran, indicating injected cells, and the red fluorescence of the internalized rhodamine-transferrin. The control-injected hepatocytes endocytosed the ligand as did the uninjected cells, whereas the anti-Dyn2T antibody-injected cells did not. Similar inhibition was found in the anti-Pan65 antibody-injected cells (not shown). Bar, 10 μ m.

Figure 2. Microinjected anti-dynamin antibodies inhibit the internalization of rhodamine-transferrin in cultured hepatocytes. Fluorescence assay for clathrin-mediated endocytosis in living cells. Cultured hepatocytes were coinjected with FITC-dextran as a marker and either heat-inactivated (*top*) or native anti-Dyn2T antibodies (*bottom*). After a 2–4-h recovery period, the cells were incubated 15 min at 37°C in DME-BSA containing 5 μ g/ml rhodamine-transferrin then rinsed and processed for fluorescence microscopy. The phase-contrast micrographs show an antibody-containing micro-needle used to inject 2–3 cells in each field (*outlined*). The corresponding fluorescence micrographs show the green

recognized a prominent band at \sim 100 kD by Western blot analysis of a rat liver cytosolic fraction (Fig. 1 *b*) and complete lysates of cultured murine hepatocytes and human skin fibroblasts (data not shown). Although an \sim 87 kD-band also was detected with the anti-Pan65 antibody in some preparations, the anti-Dyn2T antibody was specific for dynamin and did not cross react with unrelated proteins (Fig. 1 *b* and data not shown). The dynamin band was not detected with a previously characterized antibody that is specific for Dyn1 (Henley and McNiven, 1996), since Dyn1 is not expressed in epithelial cells (Fig. 1 *b*; Cook et al., 1994; Sontag et al., 1994). Finally, the control anti-kinesin antibody recognized a characteristic \sim 120 kD-band, but not the dynamin band (Fig. 1 *b*).

To test for isoform specificity, these antibodies were used to immunoprecipitate dynamin from the brain, a tissue that expresses all of the known dynamin isoforms. The immune complexes were subjected to SDS-PAGE and Western blot analysis with the purified isoform-specific antibody to Dyn1 and the anti-Dyn2T antibody. As expected, the anti-Pan61 and anti-Pan65 antibodies each coprecipitated Dyn1 and Dyn2, whereas the anti-Dyn2T antibody recognized Dyn2 predominantly and precipitated only trace amounts of Dyn1 (Fig. 1 *c*). Based on these results, the antibody reagents used in this study are predicted to provide specific tools to test the function of dynamin in vivo.

Antibodies to Dynamin Inhibit Clathrin-mediated Endocytosis

To directly test the function of dynamin in endocytic processes, we injected cultured murine hepatocytes with the anti-Pan65 and anti-Dyn2T antibodies or the respective

heat-inactivated antibodies and an anti-kinesin antibody as controls. Because dynamin has been implicated in clathrin-mediated endocytosis, we first assayed whether injected cells could internalize rhodamine-labeled transferrin (rhodamine-transferrin). This ligand is endocytosed by a clathrin-mediated pathway (Hopkins and Trowbridge, 1983; Sager et al., 1984) and has been used previously to assess the function of dynamin (Damke et al., 1994, 1995; van der Bliek et al., 1993). As shown in Fig. 2, cells injected with the heat-inactivated antibodies endocytosed rhodamine-transferrin, as did the adjacent uninjected cells. Cells injected with the anti-kinesin antibody also internalized the fluorescent ligand (data not shown, but see Fig. 3). In contrast, clathrin-mediated endocytosis was inhibited in cells that were injected with the native affinity-purified anti-Dyn2T antibody as assessed by the lack of internal rhodamine-transferrin fluorescence. Identical results were obtained in cells that were injected with the anti-Pan65 antibody. The effects of these antibody injections on clathrin-mediated endocytosis were quantitated by determining the percentage of injected cells that internalized rhodamine-transferrin (Fig. 3). As expected, we found that 77–90% of the control anti-kinesin and heat-inactivated antibody injected cells endocytosed fluorescent transferrin conjugates. In contrast, only 8–16% of the anti-Pan65 and anti-Dyn2T antibody-injected cells internalized the ligand, consistent with a greater than fourfold decrease in clathrin-mediated endocytosis.

Next we analyzed the ultrastructure of antibody-injected cells by electron microscopy to test for aberrations in plasmalemmal morphology. To discriminate between internalized vesicles and those associated with the plasma membrane, we processed cells for electron microscopy using ruthenium red in the primary and secondary fixations. This electron-dense dye stains the outer leaflet of the

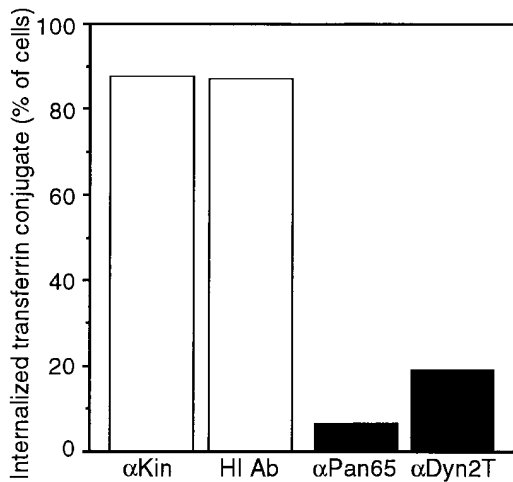


Figure 3. Quantitated inhibition of clathrin-mediated endocytosis in anti-dynamin antibody-injected hepatocytes. The clathrin-mediated endocytosis of rhodamine- and Texas red-labeled transferrin is reduced greater than fourfold in cells injected with the anti-dynamin antibodies over that in control-injected cells. Hepatocytes were injected with the anti-kinesin (α Kin; $n = 78$) and heat-inactivated (HI Ab; $n = 271$) antibodies as controls or the anti-Pan65 (α Pan65; $n = 135$) and anti-Dyn2T (α Dyn2T; $n = 457$) antibodies. Cells then were incubated with rhodamine- or Texas red-transferrin, fixed, and then processed for fluorescence microscopy as in Fig. 2. For each condition the number of injected cells that internalized the transferrin conjugate (those containing red fluorescence) was counted and expressed as a percentage of the sum of injected cells.

plasma membrane and any continuous invaginations at the time of fixation (Jollie and Triche, 1971). We observed numerous, long, ruthenium red-stained, plasmalemmal invaginations in the anti-Pan65 (data not shown) and anti-Dyn2T antibody-injected cells (Fig. 4) similar to those seen in the *shibire^{ts1}* mutant cells at the restrictive temperature (Kessell et al., 1989) and mammalian cells overexpressing a mutant dynamin (Damke et al., 1994). Densely stained, clathrin-coated pits frequently were associated with these plasmalemmal invaginations, consistent with a defect in clathrin-mediated endocytosis. Plasmalemmal invaginations that formed in control and anti-dynamin antibody-injected cells were quantitated by determining the percentage of the cell volume that contained ruthenium red-labeled membranes. Significantly, the amount of invaginated plasma membrane increased about twofold in the anti-dynamin antibody-injected cells over that found in cells that were injected with the heat-inactivated antibodies (Table I). These results confirm that Dyn2 specifically plays a role in clathrin-mediated endocytosis and demonstrate that the function of Dyn2 can be inhibited effectively in living cells through the microinjection of the anti-Pan65 and anti-Dyn2T antibodies.

Distinct Endocytic Structures Accumulate in Anti-dynamin Antibody-injected Cells

In addition to the long clathrin-coated pits that formed in the anti-dynamin antibody-injected cells, we observed many smaller 65–75-nm-diam plasmalemmal invaginations that did not have clathrin coats, but closely resembled ca-

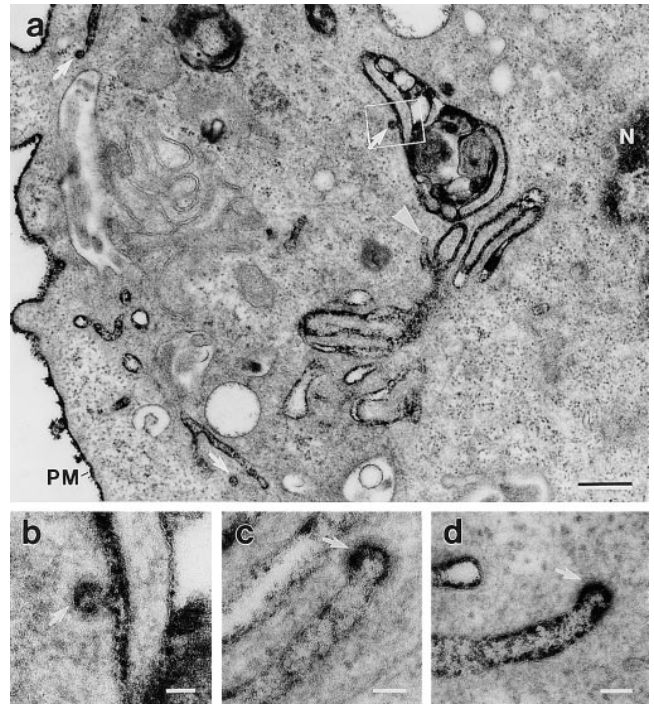


Figure 4. Microinjected anti-dynamin antibodies induce the accumulation of long clathrin-coated pits. Electron micrographs showing the long plasmalemmal invaginations and associated coated pits (arrows) that form in anti-dynamin antibody-injected cells. Hepatocytes were injected with the anti-Dyn2T antibody as in Fig. 2 and then processed for electron microscopy with ruthenium red included in the fixatives to stain the surface membranes. (a) The densely stained structures, although deep within the cytoplasm near the nucleus (N), are continuous with the plasma membrane (PM). A nonclathrin-coated bud that is connected to a plasmalemmal invagination also can be seen (arrowhead). The outlined area is shown at higher magnification in b. (b–d) The bristle-like clathrin coat can readily be seen on the distended regions, or buds, of long plasmalemmal invaginations. Similar invaginations were found when the anti-Pan65 antibody was injected, but not in cells that were injected with the control solutions (not shown). Bars: (a) 0.3 μ m; (b–d) 0.05 μ m.

veolae (Fig. 5). Caveolae (“small caves”) are specializations of the plasma membrane that are found in many different cells types (reviewed in Anderson, 1993b; Lisanti et al., 1994; Parton, 1996; Severs, 1988). These plasmalemmal vesicles were described first by conventional transmission

Table I. Relative Internal Volume of Ruthenium Red-labeled Plasmalemmal Invaginations in Antibody-injected Hepatocytes

Injected antibody	Surface invaginations* (percent cell volume)	Range (percent cell volume)	n	Increase over control (-fold)
HI Ab	0.50 \pm 0.14	0–2.62	23	1.0
α Dyn Ab	0.98 \pm 0.20 [‡]	0–5.09	34	2.0

Hepatocytes were injected with heat-inactivated antibodies as controls (HI Ab) or anti-dynamin antibodies (α Dyn Ab; anti-Pan65, $n = 27$ and anti-Dyn2T, $n = 7$), then fixed and processed for electron microscopy using ruthenium red to stain the plasma membranes as in Fig. 4. The relative internal volume of ruthenium red-labeled plasmalemmal invaginations was determined with a grid overlay on electron micrographs of complete cell profiles (n). *Values are median relative volumes \pm SEM. [‡]Using the Wilcoxon rank sum analysis this value is significantly different from the control value ($P < 0.02$; two-tailed test), whereas the values from individual data sets were not significantly different from each other.

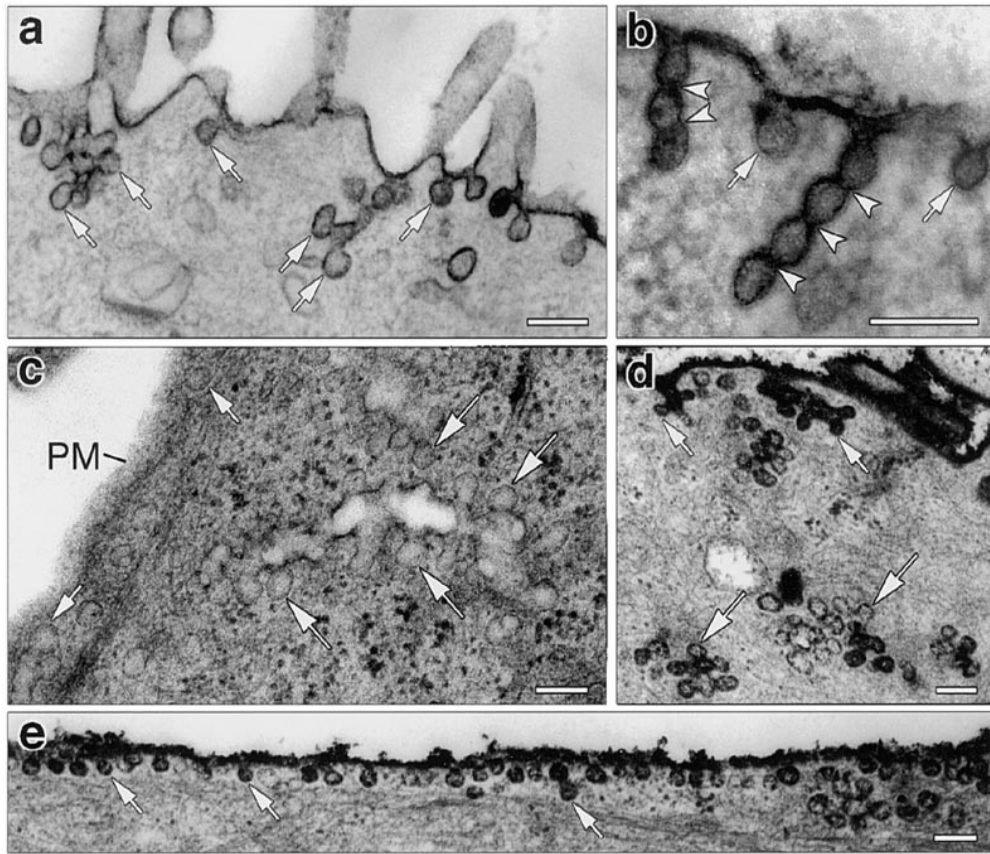


Figure 5. Accumulation of distinct endocytic structures in cultured hepatocytes injected with anti-dynamin antibodies. (a–c) Electron micrographs show typical membrane invaginations found at the surface of cells that were injected with the Dyn2-specific anti-Dyn2T antibody. Numerous budding profiles (small arrows) lacking clathrin coats and resembling caveolae were found at the plasma membrane (a and b). Long “chains” of vesicles separated by constrictions (arrowheads) also were found attached to the plasma membrane (b). In addition, clusters of multiple vesicular profiles were observed deeper within the cell (c, large arrows). Similar structures were found in the anti-Pan65 antibody-injected cells but not in the control-injected cells. (d and e) Electron micrographs of anti-Dyn2T (d) and anti-Pan65 (e) antibody-injected cells that were fixed and stained with ruthenium red as in Fig. 4. Dark vesicles reveal both surface (small arrows) and deep (large arrows) membrane invaginations that are continuous with the plasma membrane. Bars, 0.15 μm .

electron microscopy based on their characteristic ultrastructure; they are 50–85 nm in diameter, flask-shaped, and have no obvious cytoplasmic coats (Palade, G.E. 1953. *J. Appl. Physics*. 24:1424 (Abstr.); Palade and Bruns, 1968; Yamada, 1955). Although the precise cellular function of caveolae remains undefined, they have been implicated in the internalization of specific ligands, including cholera toxin (Montesano et al., 1982; Tran et al., 1987; Parton, 1994; Schnitzer et al., 1996), GPI-anchored proteins (Parton et al., 1994; Smart et al., 1994, 1995), albumin (Schnitzer et al., 1994), small proteins (Predescu et al., 1994, 1997), HLA antigens (Huet et al., 1980), and SV40 (Kartenbeck et al., 1989; Stang et al., 1997). The scission of these plasmalemmal vesicles from the plasma membrane during caveola-mediated endocytosis is dependent upon GTP hydrolysis (Schnitzer et al., 1996). Although single caveolar profiles were found normally in uninjected and control-injected cells (data not shown, but see Fig. 8), many of the caveolar profiles observed in the anti-dynamin antibody-injected cells were comprised of 3–8 vesicles arranged as complex clusters (Fig. 5 a) or long chains (Fig. 5 b). These large clusters and chains, which appear to be groups of scission-incompetent caveolae, rarely were seen in unin-

jected cells or in cells that were injected with the control solutions. Whereas many of these complex structures were linked directly to the plasma membrane (Fig. 5, a and b), others were resolved deep within the cytoplasm (Fig. 5 c). Such structures may represent plasmalemmal invaginations that extend in and out of the plane of section or truly may be internal endocytic or secretory compartments. To discriminate between these possibilities, we again used ruthenium red to stain the surface membranes as was done for examining the clathrin-coated pits shown in Fig. 4. From this staining we could resolve many darkly stained clusters of caveolae both at the plasma membrane (Fig. 5, d and e) and deeper within the cytoplasm (Fig. 5 d). We quantitated the density of caveolar invaginations at the plasma membrane and found a greater than twofold increase from 0.93 per μm in control-injected cells to 2.18 per μm in cells that were injected with the anti-Pan65 and anti-Dyn2T antibodies (Table II).

Anti-dynamin Antibodies Inhibit Caveola-mediated Uptake of Labeled Cholera Toxin B

The significantly increased density of plasmalemmal cave-

Table II. Surface Density of Caveolae in Antibody-injected Hepatocytes

Injected antibody	Caveola density*	Range	n	Total surface membrane	Fold increase
	per μm	caveolae per μm		μm	
HI Ab	0.93 ± 0.28	0.33–4.46	23	295.7	1.0
$\alpha\text{Dyn Ab}$	$2.18 \pm 0.30^{\ddagger}$	0.74–7.91	34	307.2	2.3

Hepatocytes were injected with heat-inactivated antibodies as controls (HI Ab) or the anti-dynamin antibodies ($\alpha\text{Dyn Ab}$; anti-Pan65, $n = 27$ and anti-Dyn2T, $n = 7$) then fixed and processed for electron microscopy using ruthenium red to stain the plasma membranes as in Fig. 5, *d* and *e*. The surface density of caveolae in antibody-injected hepatocytes was determined from electron micrographs of complete cell profiles (n) for each set of injections. *Values are expressed as the median density \pm SEM. \ddagger Using the Wilcoxon rank sum analysis this value differs significantly from the control value ($P < 0.001$; two-tailed test).

olae in the anti-dynamin antibody-injected cells (see Table II) is consistent with Dyn2 directly mediating the scission of caveolae at the plasma membrane. An alternative explanation is that a caveola-mediated endocytic pathway was upregulated in these injected cells in response to inhibiting the function of Dyn2. This possibility is supported by the findings of Damke et al. (1995), who showed there was an increase of fluid-phase endocytosis in cultured cells overexpressing a mutant Dyn1. To test whether caveola-mediated endocytosis was inhibited or upregulated in the anti-dynamin antibody-injected cells, we used an assay to follow in vivo the internalization of FITC–cholera toxin B.

FITC–cholera toxin B has been used previously as a tool to study caveola-based endocytic pathways (Schnitzer et al., 1996). This toxin binds to specific GM₁ glycosphingolipids at the surface of multiple cell types (Critchley et al., 1982; reviewed in Fishman, 1982*b*), where it is sequestered and internalized by nonclathrin-coated pits and vesicles that have been identified as caveolae (Montesano et al., 1982; Tran et al., 1987; Parton, 1994). The toxin then is transported to endosomes and accumulates intracellularly within perinuclear cytoplasmic compartments (Joseph et al., 1979; Montesano et al., 1982; Parton, 1994; Sandvig et al., 1996; Schnitzer et al., 1996; Tran et al., 1987). Cultured hepatocytes were injected with the native anti-Pan65 and anti-Dyn2T antibodies, and heat-inactivated antibodies or an anti-kinesin antibody were injected as controls. Cells then were labeled with FITC–cholera toxin B for 15 min at 4°C. The unbound toxin conjugate was rinsed away, and after a 2.5-h incubation at 37°C to allow the ligand to become internalized, the cells were fixed and viewed by fluorescence microscopy. To observe distinct endocytic pathways, some cells also were incubated with Texas red–labeled transferrin (Texas red–transferrin) during the last 15 min of the 2.5-h incubation. As shown in Fig. 6, FITC–cholera toxin B fluorescence was sequestered into brightly labeled cytoplasmic vesicles and perinuclear compartments of both control-injected and uninjected cells. In contrast, FITC–cholera toxin B was restricted to the plasma membrane of cells that were injected with the anti-dynamin antibodies

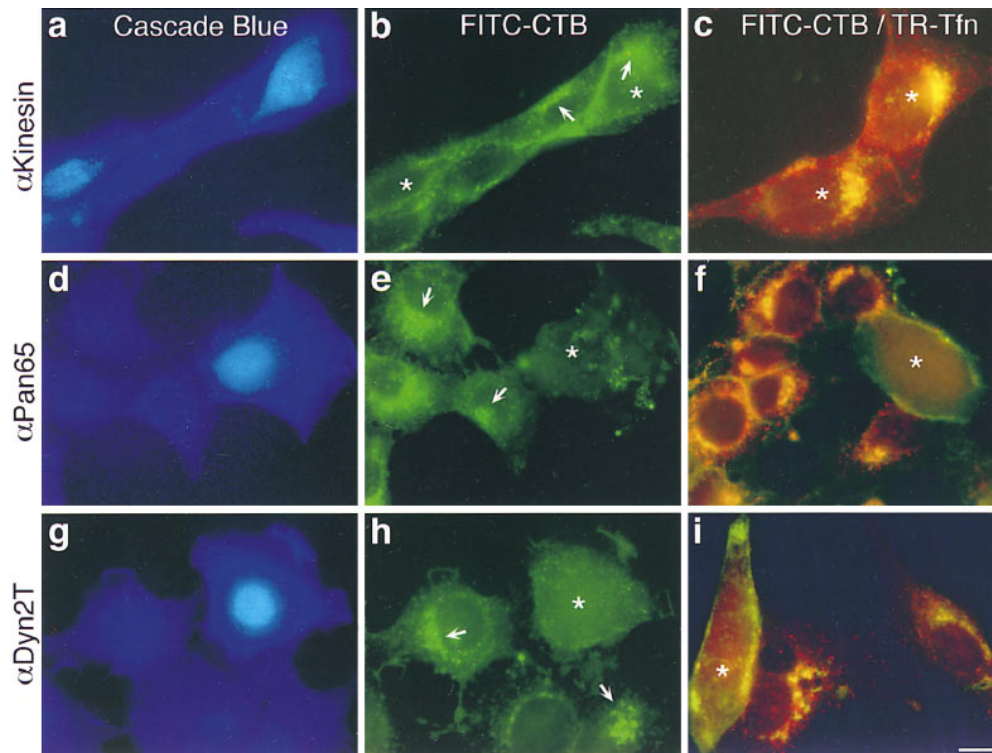


Figure 6. Microinjected anti-dynamin antibodies inhibit the internalization of FITC–cholera toxin B in living cells. Fluorescence micrographs of cultured hepatocytes injected with purified antibodies to kinesin (*a–c*) as a control, or the anti-Pan65 (*d–f*) and anti-Dyn2T (*g–i*) antibodies. Cascade blue hydrazide was included in the antibody solutions to identify injected cells (*a*, *d*, and *g*). Injected cells were incubated with FITC–cholera toxin B (FITC–CTB) at 4°C to allow binding, then rinsed and incubated in toxin-free medium for 2 h at 37°C to allow internalization. Cells were incubated an additional 30 min at 37°C in the absence (*b*, *e*, and *h*) or presence (*c*, *f*, and *i*) of Texas red–transferrin (TR–Tfn) then fixed for fluorescence microscopy as in Fig. 2. Asterisks mark injected cells. (*a–c*) In the control anti-kinesin

antibody-injected cells and in the adjacent uninjected cells bright perinuclear green fluorescence (arrows) and noticeably dark nuclei indicate that caveola-mediated endocytosis of FITC–cholera toxin B has occurred. Likewise, the punctate red fluorescence in the double-labeled cells indicates that clathrin-mediated endocytosis of Texas red–transferrin was normal. In these cells the yellow fluorescence indicates a morphological overlap of the two ligands, most likely within endosomal compartments. (*d–i*) Cells that were injected with the anti-dynamin antibodies have little internal fluorescence when compared with the adjacent uninjected cells, indicating that the endocytic uptake of both FITC–cholera toxin B and Texas red–transferrin was inhibited. Bar, 10 μm .

and did not accumulate intracellularly. These results are consistent with those of Schnitzer et al. (1996), who found a similar intracellular distribution of endocytosed FITC–cholera toxin B in control cells that was disrupted in perforated cells which were pretreated with GTP- γ S. The anti-dynamin antibody-injected cells also were devoid of internal Texas red–transferrin fluorescence, which indicates that both the internalization of caveolae and clathrin-mediated endocytosis were inhibited and demonstrates that Dyn2 participates in distinct endocytic processes in the same cell (Fig. 6). Control experiments where uninjected cells first were depleted of postassium for 2.5 h to inhibit clathrin-mediated endocytosis (Larkin et al., 1983, 1985) before the assays support the existence of these two distinct endocytic pathways in the cultured hepatocytes: FITC–cholera toxin B still was internalized normally, whereas Texas red–transferrin was not (data not shown).

The percentage of antibody-injected cells that internalized FITC–cholera toxin B was calculated to measure caveola-mediated endocytosis. Fig. 7 demonstrates that although \sim 88% of the anti-kinesin and heat-inactivated antibody-injected cells internalized FITC–cholera toxin B, this percentage dropped significantly to $<$ 20% of the cells that were injected with the anti-Pan65 and anti-Dyn2T antibodies. Thus, caveola-mediated endocytosis is reduced greater than fourfold in the anti-dynamin antibody-injected cells.

To support these findings, we examined the antibody-injected cells by electron microscopy after labeling them with HRP–cholera toxin B. First, cultured hepatocytes were injected with the anti-Pan65 and anti-Dyn2T antibodies or heat-inactivated antibodies as a control. Then cells were incubated with HRP–cholera toxin B as in the fluorescence assay, fixed, and processed for the cytochemical detection of peroxidase. The typical localization of internalized HRP–cholera toxin B in hepatocytes injected with a heat-inactivated antibody is illustrated in Fig. 8 *a*. By electron microscopy, peroxidase labeling was present in numerous endosomal structures, elements of the rough endoplasmic reticulum and the nuclear envelope, with negligible staining of the plasma membrane. A similar localization was found in the uninjected cells (data not shown). This internal distribution of the toxin conjugate is consistent with numerous reports from others using multiple cell types (Joseph et al., 1979; Montesano et al., 1982; Tran et al., 1987; Parton, 1994; Sandvig et al., 1996). In contrast, cells injected with the anti-Pan65 (Fig. 8 *b*) and anti-Dyn2T (data not shown) antibodies did not contain internal peroxidase reaction product. Instead, HRP–cholera toxin B labeling remained at the plasma membrane where it was concentrated in nonclathrin-coated caveolar profiles and grape-like caveolar clusters (Fig. 8, *c* and *d*). Little, if any labeling was detected in the endosomes, the endoplasmic reticulum, or the nuclear envelope. Thus, the anti-dynamin antibody-injected cells were able to sequester HRP–cholera toxin B within plasmalemmal caveolae but were unable to complete the internalization process. These ultrastructural studies support the earlier fluorescence assay (see Figs. 6 and 7) and morphological observations (see Fig. 5 and Table II), confirming that Dyn2 participates in the caveola-mediated endocytosis of cholera toxin B.

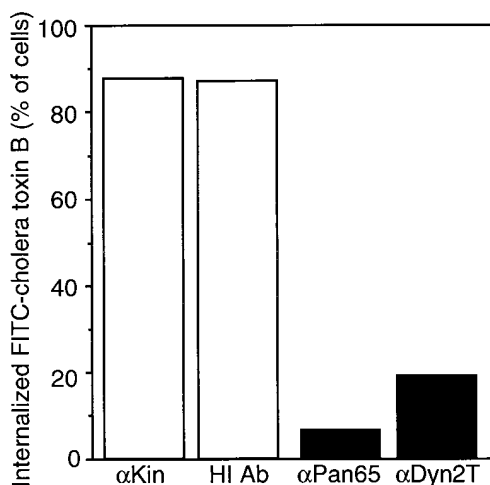


Figure 7. Quantitated inhibition of caveola-mediated endocytosis in anti-dynamin antibody-injected hepatocytes. Caveola-mediated endocytosis of FITC–cholera toxin B is reduced greater than fourfold in cells injected with the anti-dynamin antibodies over that in the control-injected cells. Hepatocytes were injected with anti-kinesin (α Kin; $n = 277$) and heat-inactivated (*HI Ab*; $n = 93$) antibodies as controls or the anti-Pan65 (α Pan65; $n = 46$) and anti-Dyn2T (α Dyn2T; $n = 184$) antibodies. Cells then were labeled with FITC–cholera toxin B, fixed and processed for fluorescence microscopy as in Fig. 6. As described in Fig. 6, the criteria for counting a cell positive for internal FITC–cholera toxin B was the presence of perinuclear green fluorescence and a dark nucleus (or nuclear “ghost”). For each condition the number of injected cells that internalized the toxin conjugate was counted and expressed as a percentage of the total.

Dynamin Associates with Caveolae

To verify that dynamin was present on caveolar membranes, we first performed immunoisolation experiments using the anti-Pan61 antibody and a control polyclonal antibody to the pIgA-R (Henley and McNiven, 1996). Antibodies were linked to paramagnetic beads and then incubated with a postnuclear membrane fraction that was obtained from the same cultured murine hepatocytes used throughout this study. Immunobeads and bound membranes were collected with a magnet, rinsed, and then subjected to SDS-PAGE and quantitative Western blot analysis using antibodies to the caveolar membrane protein caveolin (Rothberg et al., 1992; Dupree et al., 1993), the integral plasmalemmal Na^+/K^+ ATPase (Shyjan and Severson, 1989), or the α subunit of the AP-2 adaptor complex. Fig. 9 illustrates that caveolin is expressed in the cultured hepatocytes and was detected readily in the starting postnuclear membrane fraction (Fig. 9, *a*, top and *b*, lane 1). Significantly, the material isolated with the anti-Pan61 antibody contained substantial caveolin immunoreactivity, indicating that dynamin associates with caveolar membranes (Fig. 9, *a*, top and *b*, lane 2). This association was prominent, since the anti-Pan61 antibody depleted most of the caveolin that was present in the starting membrane fraction (Fig. 9, *a*, top and *b*, lane 3). In contrast, caveolar membranes were not isolated by the control anti-pIgA-R antibody since only trace amounts of caveolin were found in this immunisolated fraction (Fig. 9 *a*, top and *b*, lane 4)

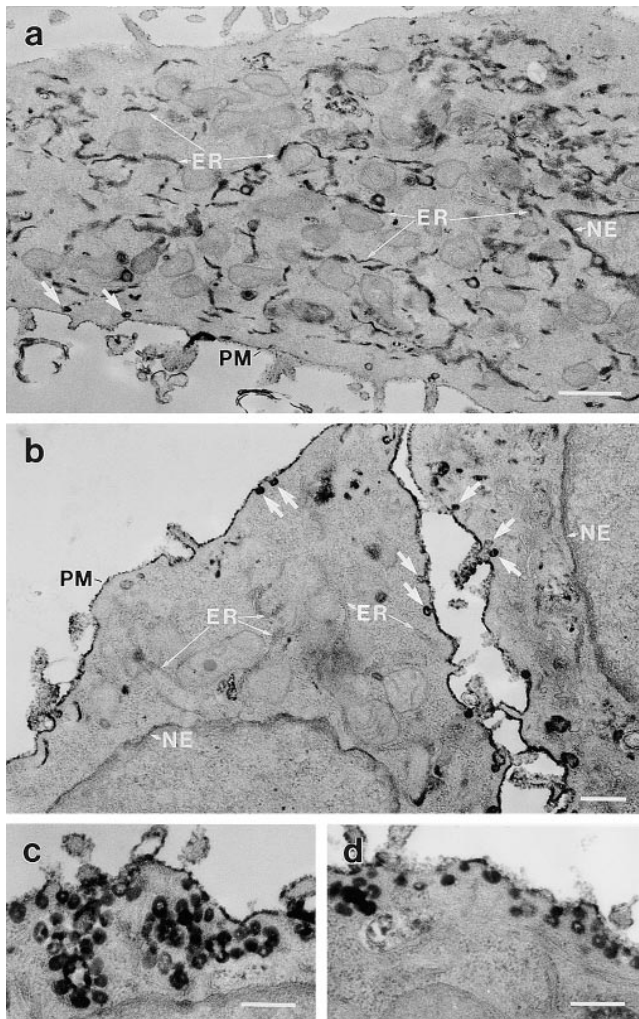


Figure 8. Anti-dynamin antibodies prevent the caveola-mediated endocytosis of HRP-cholera toxin B, as confirmed by electron microscopy. Electron micrographs show hepatocytes that were injected with either a heat-inactivated antibody as a control (a) or the anti-Pan65 antibody (b-d). After the injections, cells were incubated with HRP-cholera toxin B as in Fig. 6, fixed, then processed for diaminobenzidine cytochemistry and electron microscopy. (a) A control-injected cell showing the internal electron-dense peroxidase reaction product that is sequestered largely within elements of the rough endoplasmic reticulum (ER) and the nuclear envelope (NE), with little remaining at the plasma membrane (PM). (b-d) Cells injected with the native anti-Pan65 antibody have little, if any HRP-cholera toxin B labeling of the endosomes, the endoplasmic reticulum, and the nuclear envelope, with most of the peroxidase reaction product residing on the plasma membrane or in numerous caveolae (arrows) and grape-like caveolar clusters. Similar observations were made in cells injected with the anti-Dyn2T antibody (not shown). Bars: (a) 0.5 μm ; (b-d) 0.2 μm .

and, as expected, most of the caveolin immunoreactivity remained in the fraction that did not bind to this antibody (Fig. 9, a, top and b, lane 5). Also significant is the finding that neither the Na^+/K^+ ATPase nor the AP-2 adaptor complex were enriched in the anti-Pan61 immunisolated fraction compared with the anti-pIgA-R immunisolated fraction. This indicates that the caveolar membranes were

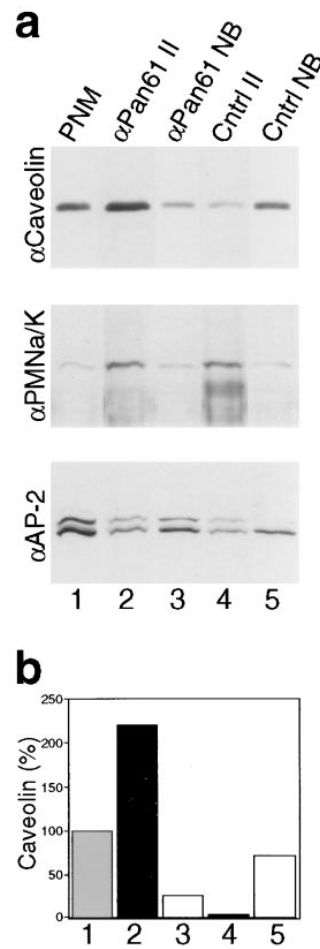


Figure 9. A dynamin antibody immunisolates caveolar membranes. Representative immunoblots (a) and densitometric analysis (b) showing that caveolar membranes can be immunisolated with an anti-dynamin antibody. (a) A starting post-nuclear membrane fraction was prepared from cultured murine hepatocytes (lane 1), and fractions were immunisolated with the anti-Pan61 (lane 2) and control anti-pIgA-R (lane 4) antibodies linked to paramagnetic beads. Immunisolated fractions were collected with a magnet, whereas material that did not bind to the anti-Pan61 (lane 3) and control anti-pIgA-R (lane 5) antibodies was pelleted by centrifugation and collected as the nonbound fractions. Fractions then were subjected to SDS-PAGE and quantitative Western blot analysis using antibodies to the caveolar membrane coat protein caveolin (top); the Na^+/K^+ ATPase as a plasmalemmal marker (middle); and α -adaptin, a marker for AP-2/clathrin coats at the plasma membrane (bottom).

substantially in the immunisolated fraction obtained with the anti-Pan61 antibody over that found in the fraction obtained with the control antibody, whereas the plasmalemmal Na^+/K^+ ATPase and the AP-2 adaptor complex are not. Similar results were found from experiments done on cultured human fibroblast membrane fractions (data not shown). (b) Quantitation of the caveolin immunoreactivity that was detected in each of the fractions described above. Western blots were subjected to densitometric analysis and the relative intensity of the caveolin band in each fraction was normalized to the starting membrane fraction, which was set at 100%. Quantitation was done on blots from at least two experiments, with similar results (not shown).

isolated directly and not by an indirect interaction with the plasma membrane or clathrin-coated pits (Fig. 9 a, middle and bottom). Immunisolations done using a postnuclear membrane fraction from cultured human fibroblasts gave similar results, indicating that the association of dynamin with caveolae is not unique to the hepatocyte cell line used in this study (data not shown).

To complement the immunolocalization experiments described above, double label immunofluorescence microscopy of cultured hepatocytes was performed. Fixed cells were processed for indirect immunocytochemistry using a monoclonal anti-caveolin antibody to label caveolae and the polyclonal anti-Pan61 antibody to localize the endogenous dynamin. Representative micrographs obtained by confocal laser scanning microscopy are shown in Fig. 10

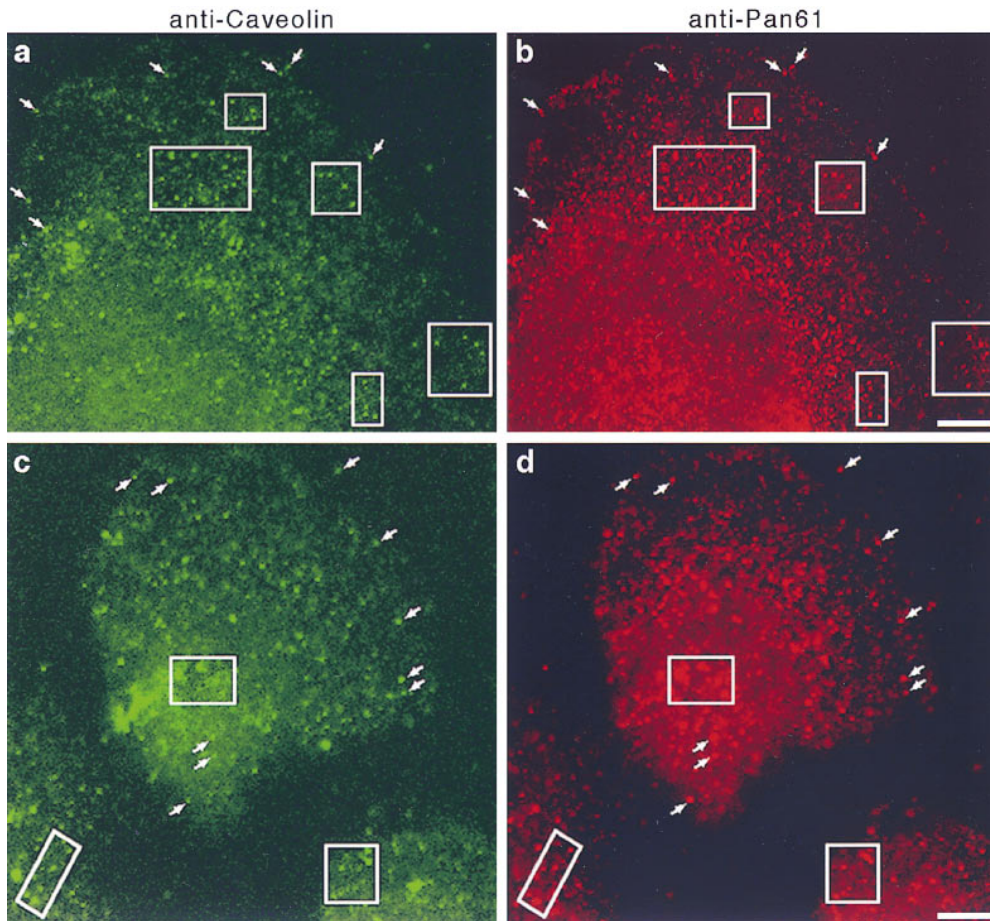


Figure 10. Dynamin localizes to caveolae in cultured hepatocytes. Fluorescence micrographs representing laser scanning confocal microscopy of cultured hepatocytes that were double labeled with a monoclonal anti-caveolin antibody (*a* and *c*) as a marker for caveolae and the polyclonal anti-Pan61 antibody (*b* and *d*) to label the endogenous dynamin. Two separate fields of cells are shown (*top* and *bottom*). A significant number of vesicular structures are labeled with both antibodies (*arrows* and *outlined areas*), indicating a colocalization of dynamin and caveolin. A similar staining pattern was obtained with the anti-Pan65 antibody but not in controls where primary antibodies were omitted (not shown). Bars, 8.0 μm .

and demonstrate the significant overlap of the two staining patterns. Although some of the caveolin and dynamin labeling remains separate, a striking colocalization on peripheral vesicles indicates that a population of caveolae is positive for dynamin. The dynamin immunoreactivity that is distinct from the caveolin labeling most likely represents a localization to clathrin-coated membranes, since double labeling with antibodies to dynamin and clathrin reveals a significant colocalization (data not shown; but see Jones et al., 1998). These results are consistent with the biochemical data presented in Fig. 9 and support the body of evidence indicating that dynamin mediates the scission of caveolae from the plasma membrane in addition to its role in clathrin-mediated endocytosis.

Discussion

In this study we tested the function of Dyn2 *in vivo* by microinjecting specific inhibitory antibodies into cultured murine hepatocytes. Using a functional assay and ultrastructural analysis, we demonstrated that cells injected with anti-dynamin antibodies did not internalize fluorescent conjugates of transferrin but rather accumulated long plasmalemmal invaginations with attached coated pits. These observations confirm that Dyn2 regulates clathrin-mediated endocytosis in epithelial cells and are consistent with the *shibire^{ts1}* phenotype (Kosaka and Ikeda, 1983b; Kessel et al., 1989; Koenig and Ikeda, 1990) and the re-

ports of others using transfected cells overexpressing a mutant dynamin (Herskovitz et al., 1993; van der Blik et al., 1993; Damke et al., 1994, 1995). Furthermore, these results demonstrate that this technique inhibits the function of the Dyn2 isoforms in living cells. By electron microscopy we observed, in addition to the clathrin-coated endocytic membranes, numerous plasmalemmal specializations resembling caveolae that also accumulated in the anti-dynamin antibody-injected cells. These plasmalemmal vesicles are distinct from clathrin-coated pits because they lack “bristle-like” coats, are 65–75 nm in diameter, and they have a characteristic omega or flask shape. Functional assays using FITC and HRP conjugates of cholera toxin B, a GM₁ glycosphingolipid-binding ligand that is internalized via a caveola-mediated process (Montesano et al., 1982; Tran et al., 1987; Parton et al., 1994; Schnitzer et al., 1996), show that cholera toxin B internalization was inhibited dramatically in the anti-dynamin antibody-injected cells. Instead of accumulating within intracellular compartments as occurred in the control-injected cells, the toxin remained concentrated within complex caveolar invaginations at the surface of the anti-dynamin antibody-injected cells. In addition, immunoprecipitation experiments and double label immunofluorescence microscopy showed that dynamin associates with caveolae directly in cultured hepatocytes. These results provide important evidence that Dyn2 mediates the internalization of caveolae. Furthermore, this study suggests that Dyn2 supports the scission of distinct endocytic vesicles within mammalian cells.

Specificity of the Anti-dynamin Antibodies Used in This Study

This investigation used distinct anti-dynamin antibodies to inhibit the function of Dyn2 in living cells. To increase the probability of a specific functional inhibition, we used affinity-purified anti-peptide antibodies that were made to two distinct regions of Dyn2. The anti-Pan61 and anti-Pan65 antibodies are to an NH₂-terminal domain that is conserved among the dynamin family, whereas the anti-Dyn2T antibody is to a COOH-terminal region that is unique to Dyn2 (Cook et al., 1994; Sontag et al., 1994). Each of the antibodies recognized a prominent ~100-kD dynamin band by Western blot analysis. We view these antibodies as remarkably sensitive and specific considering that dynamin is expressed in the liver at low levels. Indeed, few antibodies to date are able to recognize endogenous dynamin in nonneuronal cells, which is why dynamin once was considered to be brain-specific (Nakata et al., 1991; Scaife and Margolis, 1990). Of the protein sequences that are listed in the Genbank and Swiss-Prot databases, Dyn1 is the most similar to Dyn2, sharing 26–42% identity within the tail region to which the anti-Dyn2T antibody was made. Significantly, the anti-Dyn2T antibody immunoprecipitated only trace amounts of Dyn1 from the brain, and, therefore, most likely interacts exclusively with Dyn2 when injected into cultured hepatocytes. Importantly, in this study similar results were obtained with either of the native anti-Pan65 and anti-Dyn2T antibodies but not with antibodies that were heat inactivated before injection to control for artifacts resulting from the injection procedure or from incomplete dialysis of the antibody solutions. In addition, we injected an irrelevant antibody to the vesicle-associated enzyme kinesin at a similar concentration as the anti-dynamin antibodies to control for nonspecific effects of injected antibodies.

Whereas the anti-Pan61 antibody was very efficient at immunisolating caveolar membranes from a starting postnuclear membrane fraction, the anti-Pan65 and anti-Dyn2T antibodies were not. Future detailed biochemical studies will address whether the epitopes recognized by the anti-Pan65 and anti-Dyn2T antibodies are masked by interactions between the dynamin isoforms and target proteins or membranes. Importantly, however, immunofluorescence microscopy with the anti-Pan65 antibody gave a punctate labeling pattern that overlapped significantly with the caveolin labeling, similar to the anti-Pan61 antibody (data not shown, but see Fig. 10).

Role of Dyn2 in Distinct Endocytic Processes

In this report we provide morphological evidence that indicates distinct endocytic structures accumulate in anti-dynamin antibody-injected cells. The long clathrin-coated invaginations identified by electron microscopy are characteristic of an inhibition of clathrin-mediated endocytosis (Kosaka and Ikeda, 1983b; Damke et al., 1994, 1995; Kessel et al., 1989; Koenig and Ikeda, 1990; Shupliakov et al., 1997). However, the marked accumulation of aberrant clusters of nonclathrin-coated, 65–75-nm-diam plasmalemmal vesicles resembling complexes of caveolae, and the dramatic increase in the surface density of caveolae are consistent with defective severing of these endocytic or-

ganelles from the plasma membrane (Schnitzer et al., 1996). Caveolae contain a cytoplasmic coat that is not resolved readily by conventional transmission electron microscopy but can be detected by high resolution scanning electron microscopy or rapid freezing techniques (Peters et al., 1985; Rothberg et al., 1992). The integral membrane protein caveolin, also known as VIP21 (Glenney and Zokas, 1989; Glenney and Soppet, 1992; Kurzchalia et al., 1992), is a component of this cytoplasmic coat (Rothberg et al., 1992; Dupree et al., 1993) and is necessary and sufficient for the de novo generation of caveolae (Chung, K.N., P.C. Elwood, and J.E. Heuser. 1996. *Mol. Biol. Cell.* 7:277a. (Abstr.); Fra et al., 1995). This coat likely is responsible for generating the force for curvature of the plasma membrane and imparting the characteristic flask shape and 50–85 nm diam to caveolar buds. This study demonstrates that a functional dynamin isoform then is necessary for the scission of these plasmalemmal invaginations to form free internalized caveolae. Identifying other components of a “scission complex” that may coassociate with Dyn2 and caveolar membranes will be of great interest for future studies.

Until recently, it was presumed that caveolae were permanent fixtures of the plasma membrane (Bundgaard et al., 1979; Frøkjær-Jensen et al., 1988; reviewed in Severs, 1988; van Deurs et al., 1993). This feature made the function of caveolae difficult to predict, although a role in the uptake of small molecules, or potocytosis, has been described (reviewed in Anderson, 1993c). Others have hypothesized a role in cellular signal transduction (reviewed in Anderson, 1993a,b; Lisanti et al., 1994) and calcium homeostasis (Fujimoto, 1993; Schnitzer et al., 1995b). Recently, several studies have provided persuasive evidence that caveolae actively sequester and internalize specific lipids, proteins, and associated ligands through an endocytic process (reviewed in Lamaze and Schmid, 1995; Parton and Simons, 1995). Certain glycosphingolipids, including GM₁ gangliosides, are enriched in vitro in nonionic detergent-resistant membrane fractions that are similar to isolated caveolar fractions (e.g., Brown and Rose, 1992; Dupree et al., 1993; Fiedler et al., 1993; Kurzchalia et al., 1992; Schnitzer et al., 1995a). Many other studies have reported that the B subunit of cholera toxin, which specifically binds to GM₁ gangliosides, is concentrated and internalized via nonclathrin-coated pits and vesicles that are distinct from those that are associated with clathrin-mediated endocytosis (Montesano et al., 1982; Tran et al., 1987; Parton, 1994; Schnitzer et al., 1996). Recently, Parton (1994) convincingly showed that cholera toxin is internalized via a caveola-mediated process but is not enriched in clathrin-coated pits and vesicles. In support of this, we found that inhibiting clathrin-mediated endocytosis in cultured hepatocytes by potassium depletion did not prevent the internalization of a fluorescent cholera toxin B conjugate (data not shown). These distinct endocytic pathways have different kinetics, with clathrin-mediated endocytosis occurring fourfold faster than internalization by caveolae (e.g., Fishman, 1982a; Tran et al., 1987). The protein phosphatase inhibitor okadaic acid stimulates caveola-mediated endocytosis, but inhibits the formation of clathrin-coated vesicles (Parton et al., 1994). Furthermore, the sterol-binding agent filipin has no effect on clathrin-mediated endocyto-

sis yet inhibits the internalization of caveolae (Schnitzer et al., 1994). Finally, activators of protein kinase C, which do not inhibit clathrin-mediated endocytosis, prevent the formation of caveolar invaginations (Smart et al., 1994, 1995).

GTP hydrolysis is necessary for the severing of caveolar invaginations to produce discrete endocytic vesicles that are detached from the plasma membrane (Schnitzer et al., 1996). Thus, the internalization of caveolae in this respect is analogous to clathrin-mediated endocytosis, which uses the cytoplasmic coat protein clathrin to form invaginations of a characteristic size and relies on a GTP-dependent scission event to form discrete coated vesicles from the plasma membrane (Carter et al., 1993; reviewed in Robinson, 1994). Here we have shown that these two distinct pathways use the large GTPase dynamin to regulate the formation of free endocytic vesicles from specialized invaginations of the plasma membrane.

The functional experiments described here, in which the microinjected anti-dynamin antibodies inhibited the cellular uptake of cholera toxin B conjugates, provide strong support for the morphological data showing an accumulation of caveolae in these cells. Together, these results indicate that Dyn2 participates in caveola-mediated endocytosis. Our results are consistent with the observations of others who have shown that cholera toxin B is endocytosed via caveolae and trafficked to endosomes (Montesano et al., 1982; Tran et al., 1987; Parton, 1994); the Golgi apparatus (Joseph et al., 1979; Sandvig et al., 1994); and, under certain conditions, elements of the endoplasmic reticulum (Sandvig et al., 1996). Although in the latter study thapsigargin was used to induce movement to this compartment, the cultured hepatocytes used in this study apparently transport substantial amounts of the conjugated toxin back to the endoplasmic reticulum and the nuclear envelope during a 2.5-h incubation. This caveola-mediated endocytosis was much slower than clathrin-mediated endocytosis. In uninjected and control-injected cells, incubations of 1–2 h were required to accumulate the cholera toxin B conjugates intracellularly, whereas only 5–15 min were necessary to internalize the fluorescent conjugates of transferrin. Regardless, both of these endocytic processes were inhibited equally by the injected anti-dynamin antibodies. Electron microscopy revealed that in the anti-dynamin antibody-injected hepatocytes, HRP–cholera toxin B was concentrated in caveolar profiles at the plasma membrane. Because the cultured hepatocytes used in this study express caveolin, we are confident in identifying these small plasmalemmal invaginations as caveolae. In support of this, we have shown that the anti-Pan61 antibody immunisolates caveolin-containing membranes directly and not by an indirect association with the plasma membrane. Furthermore, using this same antibody and an anti-caveolin antibody we have performed double label immunofluorescence microscopy of cultured hepatocytes to show that dynamin localizes to caveolae. Thus, we have concluded that anti-dynamin antibodies inhibit caveola-mediated processes based on multiple criteria: first, the characteristic shape and size of the accumulated structures; second, the fact that toxin-containing invaginations are not clathrin-coated and that toxin conjugates are internalized normally when clathrin-mediated endocytosis is inhibited by potassium depletion; third, the distinct time

frame in which ligands for clathrin-mediated and caveola-mediated pathways are internalized; fourth, results from the immunoisolation experiments and double label immunofluorescence microscopy that indicate that dynamin associates directly with caveolae; and fifth, and most importantly, the numerous careful studies published by others demonstrating the internalization of cholera toxin by caveolae (Montesano et al., 1982; Tran et al., 1987; Parton, 1994; Schnitzer et al., 1996). Finally, our results are consistent with those of Schnitzer and coworkers (Oh et al., 1998), who have used an *in vitro* assay to demonstrate that a dynamin-depleted cytosolic fraction does not support the severing of caveolae from isolated plasma membrane fractions until additional exogenous dynamin is added back to the assay.

Before this study, the answer to whether dynamin participated in endocytic pathways other than clathrin-mediated endocytosis was not clear (see Artalejo et al., 1995; Urrutia et al., 1997). Observations from cells of the *shibire^{ts1}* mutants indicate that fluid-phase endocytosis is completely inhibited at the restrictive temperature (Kessel et al., 1989; Kosaka and Ikeda, 1983a,b). Studies of transfected epithelial cells overexpressing a mutant Dyn1 isoform, however, have indicated that dynamin functions in clathrin-mediated endocytosis specifically and not in other forms of fluid-phase endocytosis (Damke et al., 1994, 1995; Herskovitz et al., 1993). In fact, fluid-phase endocytosis actually was upregulated in these cells in response to the inhibition of clathrin-mediated endocytosis (Damke et al., 1995). Significantly, like the *shibire* gene mutation, we have found that the anti-dynamin antibodies used in this study inhibit fluid-phase endocytosis in mammalian cells (Henley, J.R., and M.A. McNiven, manuscript in preparation) in addition to their effect on clathrin- and caveola-mediated endocytosis. Because of alternative splicing of the mRNA, Dyn2 is expressed as at least four isoenzymes in epithelial cells; therefore, it is possible that the microinjected anti-dynamin antibodies are inhibiting dynamin isoforms that an overexpressed mutant Dyn1 isoform would not. Certainly, defining the precise dynamin isoforms which participate in these distinct endocytic processes will prove interesting.

We thank Dr. Anthony Windebank and Dr. Peter Wollen for help with statistical analyses and Dr. David Zacharias for critical comments on the manuscript. We also are grateful to Dr. Jan Schnitzer for sharing unpublished results.

J.R. Henley is the recipient of an American Liver Foundation Student Research Fellowship. This work was supported by National Institutes of Health grants to M.A. McNiven.

Received for publication 8 July 1997 and in revised form 1 December 1997.

References

- Anderson, R.G.W. 1993a. Caveolae: where incoming and outgoing messengers meet. *Proc. Natl. Acad. Sci. USA*. 90:10909–10913.
- Anderson, R.G.W. 1993b. Plasmalemmal caveolae and GPI-anchored membrane proteins. *Curr. Opin. Cell Biol.* 5:647–652.
- Anderson, R.G.W. 1993c. Potocytosis of small molecules and ions by caveolae. *Trends Cell Biol.* 3:69–72.
- Anderson, R.G.W., M.S. Brown, and J.L. Goldstein. 1977. Role of the coated endocytic vesicle in the uptake of receptor bound low density lipoprotein in human fibroblasts. *Cell*. 10:351–364.
- Anderson, R.G.W., B.A. Kamen, K.G. Rothberg, and S.W. Lacey. 1992. Potocytosis: sequestration and transport of small molecules by caveolae. *Science*.

- Artalejo, C.R., J.R. Henley, M.A. McNiven, and H.C. Palfrey. 1995. Rapid endocytosis coupled to exocytosis in adrenal chromaffin cells involves Ca^{2+} , GTP and dynamin but not clathrin. *Proc. Natl. Acad. Sci. USA*. 92:8328-8332.
- Brown, D.A., and J.K. Rose. 1992. Sorting of GPI-anchored proteins to glycolipid-enriched membrane subdomains during transport to the apical cell surface. *Cell*. 68:533-544.
- Bundgaard, M., J. Frøkjær-Jensen, and C. Crone. 1979. Endothelial plasmalemmal vesicles as elements in a system of branching invaginations from the cell surface. *Proc. Natl. Acad. Sci. USA*. 76:6439-6442.
- Carter, L.L., T.E. Redelmeier, L.A. Woollenweber, and S.L. Schmid. 1993. Multiple GTP-binding proteins participate in clathrin-coated vesicle-mediated endocytosis. *J. Cell Biol.* 120:37-45.
- Chen, M.S., R.A. Obar, C.C. Schroeder, T.W. Austin, C.A. Poodry, S.C. Wadsworth, and R.B. Vallee. 1991. Multiple forms of dynamin are encoded by *shibire*, a *Drosophila* gene involved in endocytosis. *Nature*. 351:583-586.
- Cook, T.A., R. Urrutia, and M.A. McNiven. 1994. Identification of dynamin 2, an isoform ubiquitously expressed in rat tissues. *Proc. Natl. Acad. Sci. USA*. 91:644-648.
- Cook, T., K. Mesa, and R. Urrutia. 1996. Three dynamin-encoding genes are differentially expressed in developing rat brain. *J. Neurochem.* 67:927-931.
- Critchley, D.R., C.H. Streuli, S. Kellie, and B. Patel. 1982. Characterization of the cholera toxin receptor on BALB/c 3T3 cells as a ganglioside similar to, or identical with, ganglioside GM1. No evidence for galactoproteins with receptor activity. *Biochem. J.* 204:209-219.
- Damke, H., T. Baba, D.E. Warnock, and S.L. Schmid. 1994. Induction of mutant dynamin specifically blocks endocytic coated vesicle formation. *J. Cell Biol.* 127:915-934.
- Damke, H., T. Baba, A.M. van der Blik, and S.L. Schmid. 1995. Clathrin-independent pinocytosis is induced in cells overexpressing a temperature-sensitive mutant of dynamin. *J. Cell Biol.* 131:69-80.
- De Camilli, P., K. Takei, and P.S. McPherson. 1995. The function of dynamin in endocytosis. *Curr. Opin. Neurobiol.* 5:559-565.
- Dupree, P., R.G. Parton, G. Raposo, T.V. Kurzchalia, and K. Simons. 1993. Caveolae and sorting in the trans-Golgi network of epithelial cells. *EMBO (Eur. Mol. Biol. Organ.) J.* 12:1597-1605.
- Fiedler, K., T. Kobayashi, T.V. Kurzchalia, and K. Simons. 1993. Glycosphingolipid-enriched detergent-insoluble complexes in protein sorting in epithelial cells. *Biochemistry*. 32:6365-6373.
- Fishman, P.H. 1982a. Internalization and degradation of cholera toxin by cultured cells: relationship to toxin action. *J. Cell Biol.* 93:860-865.
- Fishman, P.H. 1982b. Role of membrane gangliosides in the binding and action of bacterial toxins. *J. Membr. Biol.* 69:85-97.
- Fra, A.M., E. Williamson, K. Simons, and R.G. Parton. 1995. De novo formation of caveolae in lymphocytes by expression of VIP21-caveolin. *Proc. Natl. Acad. Sci. USA*. 92:8655-8659.
- Froekjaer-Jensen, J., R.C. Wagner, S.B. Andrews, P. Hagman, and T.S. Reese. 1988. Three-dimensional organization of the plasmalemmal vesicular system in directly frozen capillaries of the rete mirabile in the swim bladder of the eel. *Cell Tissue Res.* 254:17-24.
- Fujimoto, T. 1993. Calcium pump of the plasma membrane is localized in caveolae. *J. Cell Biol.* 120:1147-1157.
- Glenny, J.R., and L. Zokas. 1989. Novel tyrosine kinase substructures from Rous sarcoma virus-transformed cells are present in the membrane skeleton. *J. Cell Biol.* 108:2401-2408.
- Glenny, J.R., and D. Soppet. 1992. Sequence and expression of caveolin, a protein component of caveolae plasma membrane domains phosphorylated on tyrosine in Rous sarcoma virus-transformed fibroblasts. *Proc. Natl. Acad. Sci. USA*. 89:10517-10521.
- Goldstein, J.L., R.G.W. Anderson, and M.S. Brown. 1979. Coated pits, coated vesicles and receptor mediated endocytosis. *Nature*. 297:678-685.
- Goldstein, J.L., M.S. Brown, R.G.W. Anderson, D.W. Russell, and W.J. Schneider. 1985. Receptor-mediated endocytosis: concepts emerging from the LDL receptor system. *Annu. Rev. Cell Biol.* 1:1-39.
- Grigliatti, T.A., L. Hall, R. Rosenbluth, and D.T. Suzuki. 1973. Temperature-sensitive mutations in *Drosophila melanogaster* XV: a selection of immobile adults. *Mol. Gen. Genet.* 120:107-114.
- Henley, J.R., and M.A. McNiven. 1996. Association of a dynamin-like protein with the Golgi apparatus in mammalian cells. *J. Cell Biol.* 133:761-775.
- Herskovits, J.S., C.C. Burgess, R.A. Obar, and R.B. Vallee. 1993. Effects of mutant rat dynamin on endocytosis. *J. Cell Biol.* 122:565-578.
- Hopkins, C.R., and I.S. Trowbridge. 1983. Internalization and processing of transferrin and the transferrin receptor in human carcinoma A431 cells. *J. Cell Biol.* 97:508-521.
- Howell, K.E., R. Schmid, J. Ugelstad, and J. Gruenberg. 1989. Immunolocalization using magnetic solid supports: subcellular fractionation for cell-free functional studies. In *Methods in Cell Biology*. A.M. Tartakoff, editor. Academic Press, San Diego, CA. 265-292.
- Huet, C., J.F. Ash, and S.J. Singer. 1980. The antibody-induced clustering and endocytosis of HLA antigens on cultured human fibroblasts. *Cell*. 21:429-438.
- Jollie, W.P., and T.J. Triche. 1971. Ruthenium labeling of micropinocytotic activity in the rat visceral yolk-sac placenta. *J. Ultrastruct. Res.* 35:541-553.
- Jones, S.M., K.E. Howell, J.R. Henley, H. Cao, and M.A. McNiven. 1998. Role of dynamin in the formation of transport vesicles from the trans-Golgi network. *Science*. 279:573-577.
- Joseph, K.C., A. Stieber, and N.K. Gonatas. 1979. Endocytosis of cholera toxin in GERL-like structures of murine neuroblastoma cells pretreated with GM1 ganglioside. *J. Cell Biol.* 81:543-554.
- Kartenbeck, J., H. Stukenbrok, and A. Helenius. 1989. Endocytosis of simian virus 40 into the endoplasmic reticulum. *J. Cell Biol.* 109:2721-2729.
- Kessell, I., B.D. Holst, and T.F. Roth. 1989. Membranous intermediates in endocytosis are labile, as shown in a temperature-sensitive mutant. *Proc. Natl. Acad. Sci. USA*. 86:4968-4972.
- Koenig, J.H., and K. Ikeda. 1989. Disappearance and reformation of synaptic vesicle membrane upon transmitter release observed under reversible blockage of membrane retrieval. *J. Neurosci.* 9:3844-3860.
- Koenig, J.H., and K. Ikeda. 1990. Transformational process of the endosomal compartment in nephrocytes of *Drosophila melanogaster*. *Cell Tissue Res.* 262:233-244.
- Kosaka, T., and K. Ikeda. 1983a. Possible temperature-dependent blockage of synaptic vesicle recycling induced by a single gene mutation in *Drosophila*. *J. Neurobiol.* 14:207-225.
- Kosaka, T., and K. Ikeda. 1983b. Reversible blockage of membrane retrieval and endocytosis in the garland cell of the temperature-sensitive mutant of *Drosophila melanogaster*, *shibire^{ts1}*. *J. Cell Biol.* 97:499-507.
- Kurzchalia, T.V., P. Dupree, R.G. Parton, R. Kellner, H. Virta, M. Lehnert, and K. Simons. 1992. VIP21, a 21-kD membrane protein is an integral component of trans-Golgi network-derived transport vesicles. *J. Cell Biol.* 118:1003-1014.
- Laemmli, U.K. 1970. Cleavage of structural proteins during the assembly of the head of bacteriophage T₄. *Nature*. 227:680-685.
- Larkin, J.M., M.S. Brown, J.L. Goldstein, and R.G. Anderson. 1983. Depletion of intracellular potassium arrests coated pit formation and receptor-mediated endocytosis in fibroblasts. *Cell*. 33:273-285.
- Larkin, J.M., W.C. Donzell, and R.G. Anderson. 1985. Modulation of intracellular potassium and ATP: effects on coated pit function in fibroblasts and hepatocytes. *J. Cell. Physiol.* 124:372-378.
- Lamaze, C., and S.L. Schmid. 1995. The emergence of clathrin-independent pinocytotic pathways. *Curr. Opin. Cell Biol.* 7:573-580.
- Lisanti, M.P., P.E. Scherer, Z.-L. Tang, and M. Sargiacomo. 1994. Caveolae, caveolin and caveolin-rich membrane domains: a signalling hypothesis. *Trends Cell Biol.* 4:231-235.
- Montesano, R., J. Roth, A. Robert, and L. Orci. 1982. Non-coated membrane invaginations are involved in binding and internalization of cholera and tetanus toxins. *Nature*. 296:651-653.
- Nakata, T., A. Iwamoto, Y. Noda, R. Takemura, H. Yoshikura, and N. Hirokawa. 1991. Predominant and developmentally regulated expression of dynamin in neurons. *Neuron*. 7:461-469.
- Nakata, T., R. Takemura, and N. Hirokawa. 1993. A novel member of the dynamin family of GTP-binding proteins is expressed specifically in the testis. *J. Cell Sci.* 105:1-5.
- Obar, R.A., C.A. Collins, J.A. Hammarback, H.S. Shpetner, and R.B. Vallee. 1990. Molecular cloning of the microtubule-associated mechanochemical enzyme dynamin reveals homology with a new family of GTP-binding proteins. *Nature*. 347:256-261.
- Oh, P., D.P. McIntosh, and J.E. Schnitzer. 1998. Dynamin at the neck caveolae mediates their budding to form transport vesicles by GTP-driven fission from the plasma membrane of endothelium. *J. Cell Biol.* 141:101-114.
- Palade, G.E., and R.R. Bruns. 1968. Structural modulation of plasmalemmal vesicles. *J. Cell Biol.* 37:633-649.
- Parton, R.G. 1994. Ultrastructural localization of gangliosides; GM₁ is concentrated in caveolae. *J. Histochem. Cytochem.* 42:155-166.
- Parton, R.G. 1996. Caveolae and caveolins. *Curr. Opin. Cell Biol.* 8:542-548.
- Parton, R.G., and K. Simons. 1995. Digging into caveolae. *Science*. 269:1398-1399.
- Parton, R.G., B. Joggerst, and K. Simons. 1994. Regulated internalization of caveolae. *J. Cell Biol.* 127:1199-1215.
- Patek, P.O., J.L. Collins, and M. Cohn. 1978. Transformed cell lines susceptible or resistant to in vivo surveillance against tumorigenesis. *Nature*. 276:510-511.
- Pearse, B.M.F., and M.S. Robinson. 1990. Clathrin, adaptors and sorting. *Annu. Rev. Cell Biol.* 6:151-171.
- Peters, K.-R., W. Carley, and G.E. Palade. 1985. Endothelial plasmalemmal vesicles have a characteristic striped bipolar surface structure. *J. Cell Biol.* 101:2233-2238.
- Poodry, C.A., and L. Edgar. 1979. Reversible alteration in the neuromuscular junctions of *Drosophila melanogaster* bearing a temperature-sensitive mutation, *shibire*. *J. Cell Biol.* 81:520-527.
- PreDESCU, D., R. Horvat, S. PreDESCU, and G.E. Palade. 1994. Transcytosis in the continuous endothelium of the myocardial microvasculature is inhibited by N-ethylmaleimide. *Proc. Natl. Acad. Sci. USA*. 91:3014-3018.
- PreDESCU, D., D.N. PreDESCU, and G.E. Palade. 1997. Plasmalemmal vesicles function as transcytotic carriers for small proteins in the continuous endothelium. *Am. J. Physiol.* 41:937-949.
- Robinson, S.A., W. Carley, and G.E. Palade. 1994. The role of clathrin, adaptors and dynamin in endocytosis. *Curr. Opin. Cell Biol.* 6:538-544.
- Robinson, P.J., J.-P. Liu, K.A. Powell, E.M. Fykse, and T.C. Südhof. 1994. Phosphorylation of dynamin I and synaptic-vesicle recycling. *Trends Neurosci.* 17:348-353.
- Rothberg, K.G., J.E. Heuser, W.C. Donzell, Y.-S. Ying, J.R. Glenny, and R.G.W. Anderson. 1992. Caveolin, a protein component of caveolae mem-

- brane coats. *Cell*. 68:673–682.
- Sager, P.R., P.A. Brown, and R.D. Berlin. 1984. Analysis of transferrin recycling in mitotic and interphase HeLa cells by quantitative fluorescence microscopy. *Cell*. 39:275–282.
- Sandvig, K., M. Ryd, O. Garred, E. Schweda, P.K. Holm, and B. van Deurs. 1994. Retrograde transport from the Golgi complex to the ER of both Shiga toxin and the nontoxic Shiga B-fragment is regulated by butyric acid and cAMP. *J. Cell Biol.* 126:53–64.
- Sandvig, K., and B. van Deurs. 1994. Endocytosis without clathrin. *Trends Cell Biol.* 4:275–277.
- Sandvig, K., O. Garred, and B. van Deurs. 1996. Thapsigargin-induced transport of cholera toxin to the endoplasmic reticulum. *Proc. Natl. Acad. Sci. USA*. 93:12339–12343.
- Scaife, R., and R.L. Margolis. 1990. Biochemical and immunochemical analysis of rat brain dynamin interaction with microtubules and organelles in vivo and in vitro. *J. Cell Biol.* 111:3023–3033.
- Schnitzer, J.E., P. Oh, E. Pinney, and J. Allard. 1994. Filipin-sensitive caveolae-mediated transport in endothelium: reduced transcytosis, scavenger endocytosis, and capillary permeability of select macromolecules. *J. Cell Biol.* 127:1217–1232.
- Schnitzer, J.E., D.P. McIntosh, A.M. Dvorak, J. Liu, and P. Oh. 1995a. Separation of caveolae from associated microdomains of GPI-anchored proteins. *Science*. 269:1435–1439.
- Schnitzer, J.E., P. Oh, B.S. Jacobson, and A.M. Dvorak. 1995b. Caveolae from luminal plasmalemma of rat lung endothelium: microdomains enriched in caveolin, Ca (2+)-ATPase, and inositol trisphosphate receptor. *Proc. Natl. Acad. Sci. USA*. 92:1759–1763.
- Schnitzer, J.E., P. Oh, and D.P. McIntosh. 1996. Role of GTP hydrolysis in fission of caveolae directly from plasma membranes. *Science*. 274:239–242.
- Severs, N.J. 1988. Caveolae: static in-pocketings of the plasma membrane, dynamic vesicles or plain artifact? *J. Cell Sci.* 90:341–348.
- Shpetner, H.S., and R.B. Vallee. 1989. Identification of dynamin, a novel mechanochemical enzyme that mediates interactions between microtubules. *Cell*. 59:421–432.
- Shupliakov, O., P. Low, D. Grabs, H. Gad, H. Chen, C. David, K. Takei, P. De Camilli, and L. Brodin. 1997. Synaptic vesicle endocytosis impaired by disruption of dynamin-SH3 domain interactions. *Science*. 276:259–263.
- Shyjan, A.W., and R. Levenson. 1989. Antisera specific for the alpha 1, alpha 2, alpha 3, and beta subunits of the Na,K-ATPase: differential expression of alpha and beta subunits in rat tissue membranes. *Biochemistry*. 28:4531–4535.
- Smart, E.J., D.C. Foster, Y.-S. Ying, B.A. Kamen, and R.G.W. Anderson. 1994. Protein kinase C activators inhibit receptor-mediated potocytosis by preventing internalization of caveolae. *J. Cell Biol.* 124:307–313.
- Smart, E.J., Y.-S. Ying, and R.G.W. Anderson. 1995. Hormonal regulation of caveolae internalization. *J. Cell Biol.* 131:929–938.
- Sontag, J.-M., E.M. Fykse, Y. Ushkaryov, J.-P. Liu, P.J. Robinson, and T.C. Südhof. 1994. Differential expression and regulation of multiple dynamins. *J. Biol. Chem.* 269:4547–4554.
- Stang, E., J. Kartenbeck, and R.G. Parton. 1997. Major histocompatibility complex class I molecules mediate association of SV40 with caveolae. *Mol. Biol. Cell*. 8:47–57.
- Takei, K., P.S. McPherson, S.L. Schmid, and P. De Camilli. 1995. Tubular membrane invaginations coated by dynamin rings are induced by GTP-γS in nerve terminals. *Nature*. 374:186–190.
- Towbin, H., T. Staehelin, and J. Gordon. 1979. Electrophoretic transfer of proteins from polyacrylamide gels to nitrocellulose sheets: procedure and some applications. *Proc. Natl. Acad. Sci. USA*. 76:4350–4354.
- Tran, D., J.L. Carpentier, F. Sawano, P. Gorden, and L. Orci. 1987. Ligands internalized through coated or noncoated invaginations follow a common intracellular pathway. *Proc. Natl. Acad. Sci. USA*. 84:7957–7961.
- Urrutia, R., J.R. Henley, T. Cook, and M.A. McNiven. 1997. The dynamins: Redundant or distinct functions for an expanding family of related GTPases? *Proc. Natl. Acad. Sci. USA*. 94:377–384.
- Vale, R.D., T.S. Reese, and M.P. Sheetz. 1985. Identification of a novel force-generating protein, kinesin, involved in microtubule-based motility. *Cell*. 42:39–50.
- van der Blik, A.M., and E.M. Meyerowitz. 1991. Dynamin-like protein encoded by the *Drosophila shibire* gene associated with vesicular traffic. *Nature*. 351:411–414.
- van der Blik, A.M., T.E. Redelmeier, H. Damke, E.J. Tisdale, E.M. Meyerowitz, and S.L. Schmid. 1993. Mutations in human dynamin block an intermediate stage in coated vesicle formation. *J. Cell Biol.* 122:553–563.
- van Deurs, N., P.K. Holm, K. Sandvig, and S.H. Hansen. 1993. Are caveolae involved in endocytosis? *Trends Cell Biol.* 3:241–249.
- Warnock, D.E., and S.L. Schmid. 1996. Dynamin GTPase, a force-generating molecular switch. *BioEssays*. 18:885–893.
- Watts, C., and M. Marsh. 1992. Endocytosis: what goes in and how. *J. Cell Sci.* 103:1–8.
- Yamada, E. 1955. The fine structure of the gall bladder epithelium of the mouse. *J. Biophys. Biochem. Cytol.* 1:445–458.